Mathematical Biosciences and Engineering

https://www.aimspress.com/journal/mbe

MBE, 22(6): 1428–1463.
DOI: 10.3934/mbe.2025054
Received: 08 December 2024
Revised: 15 April 2025
Accepted: 18 April 2025
Published: 13 May 2025

Research article

Modeling the effects of lethal and non-lethal predation on the dynamics of tick-borne disease

Kwadwo Antwi-Fordjour[1], Folashade B. Agusto[2,4,*] and Isabella Kemajou-Brown[3]

[1] Mathematics and Computer Science, Samford University, Birmingham, AL, USA
[2] Ecology and Evolutionary Biology, University of Kansas, Lawrence, KS, USA
[3] Mathematics - Actuarial Science Program, Morgan State University, Baltimore, MD, USA
[4] Mathematics and Applied Mathematics, North-West University, Potchefstroom South Africa

* **Correspondence:** Email: fbagusto@gmail.com.

Abstract: Tick-borne illnesses are transmitted to mammals like rodents and deer by infected ticks. These illnesses have shown dramatic increase in recent times, thereby increasing public health risk in the United States. Additionally, these mammals can be impacted by predation and the fear of their predators. In this study, we modeled the lethal and non-lethal effect of predation of the mammals on the dynamics of tick-borne disease using *ehrlichiosis* as our model disease system. Results of the theoretical analysis of reduced form of the model indicate that the model equilibria are stable when the tick fecundity and mortality rates are not host dependent. Furthermore, predator-induced fear and predator attack rates are two of the significant parameters of the model outputs from the sensitivity analysis carried out. Numerical simulation of the model shows that the combined impact of both lethal and non-lethal predation sets off a cascading chain reaction leading to a corresponding reduction in the prey and tick populations; in particular there are more infected larvae when infected prey population are low and few infected larvae when there are more infected prey. Similar dynamics was observed for the infected nymphs and adult ticks and infected predator population. Furthermore as the fear of the predator increases, the prey population reduces which subsequently lead to a decrease in the tick populations and subsequently disease in the community.

Keywords: tick-borne disease; ehrlichia chaffeensis; lethal and non-lethal effect of predation; sensitivity analysis; amblyomma americanum

1. Introduction

Ehrlichiosis, formally known as human monocytic *ehrlichiosis*, was recognized as a human disease in the late 1980s; however, official reporting by the CDC on the disease began in 2000 [1, 2]. Ca-

nine *ehrlichiosis*, a disease caused by the *Ehrlichia bacteria*, has received particular attention due to its influence on the health of domesticated dogs. These illnesses, which are transmitted to people by tick bites, pose a substantial danger to world health due to their potential for broad transmission and complex ecological dynamics. *Ehrlichia ewingii, Ehrlichia muris eauclairensis*, and *Ehrlichia chaffeensis* are bacterial species belonging to the class *Ehrlichiosis*. Among these, *Ehrlichia chaffeensis* is the most prevalent in the United States [2]. The bacterium responsible for *ehrlichiosis* is transmitted to humans primarily by *Amblyomma americanum*, which is of significant concern in the United States not only due to its extremely aggressive and somewhat indiscriminate biting behavior throughout all three life stages, but also because of its potential to transmit several bacteria known to cause diseases in humans [3].

Amblyomma americanum, commonly known as the lone star tick, is widely distributed across the eastern and central United States, with a range that has expanded due to climate change and habitat alterations [4,5]. It thrives in wooded areas, grasslands, and dense brush, where it can easily find hosts. The tick's life cycle consists of four stages, egg, larva, nymph, and adult, each requiring a blood meal to progress to the next stage [6]. *A. americanum* feeds on a variety of animals, including mammals, birds, and reptiles. Larvae and nymphs feed on small mammals such as rodents and rabbits [7], while adult ticks feed on large mammals such as foxes and coyotes but they primarily rely on white-tailed deer as their main hosts [8]. Coyotes, foxes, and owl are predatory animals that feed on small animals such as rabbits and rodents [9].

Extensive research has been conducted on the role of host abundance and tick ecology in disease transmission (see [10–13] and references therein); however, the impact of predation — both lethal (direct consumption of hosts) and non-lethal (behavioral and physiological changes in host populations due to predation risk) — remains less explored in mathematical models. Fear of predation can lead to a range of behavioral, physiological, and ecological responses in prey populations. The effect of these responses on the prey population and disease dynamics can be as significant as direct predation itself [14]. For instance, the fear of predators can alter host behavior, leading to reduced foraging and movement, which may decrease tick-host contact rates [15,16]. Chronic stress from predation risk can suppress host immune responses, potentially increasing their susceptibility to infection [17].

Changes in habitat use due to predator presence may modify tick-host encounter rates, either reducing or amplifying disease transmission [16]. Prey-predator interactions are fundamental drivers of ecosystem dynamics, with cascading effects that can ripple through entire food webs [18, 19]. Wang et al. [20] explore the fear effect in prey-predator interactions, revealing how the perception of predation risk can influence prey behavior and, by extension, disease transmission dynamics. This insight broadens our understanding of the non-lethal effects of predation.

Some recent studies have shed light on how the non-lethal effects of predation affect disease dynamics. In this context, Hossain et al. [21] observed that fear can eliminate chaotic oscillations of their proposed system by either making the endemic equilibrium regular (stable equilibium point or stable limit cycle) or moving it towards the disease-free state. Recently, Zhang [22] investigated the effect of the fear factor on an eco-epidemiological system with a standard incidence rate and found that an increase in the level of fear changed a disease-free equilibrium from unstable to stable. Moreover, the study by Pribadi and Chalasani [23] delves into fear conditioning in invertebrates, opening up new avenues for understanding the psychological and behavioral aspects of prey species when confronted with predation threats. However, the intricate relationship between prey-predator interactions, fear, and

tick-borne diseases has not been comprehensively explored. This gap in our knowledge highlights the critical need for further investigation on how ecological factors like prey-predator interactions and fear responses influence disease dynamics. To effectively mitigate tick-borne diseases, we must understand how prey-predator interactions, mediated by fear, impact disease prevalence in ticks.

The goal of this study is to understand the complex interplay between lethal and non-lethal predation on the dynamics of tick-borne diseases with the aim of addressing the following specific research questions:

1. What are the cascading effects of fear within ecosystems, and how do they influence tick abundance, prey behavior, and ultimately, disease transmission dynamics?
2. Can fear-induced changes in host behavior and predator dynamics serve as effective tools in managing tick-borne disease risk within a given ecosystem?

The rest of the paper is organized as follows: in Section 2, we begin by formulating the ticks-prey-predator dynamics with disease.

In order to capture the intricacies of *Amblyomma Americanum* ticks' life cycle, we classify the ticks into their different life stages and explore stability analysis and sensitivity analyzes of the resulting model. Moving into Section 3, we use a reduced version of the disease model following some stated assumption and subsequently carry out the stability. In Section 5, we carry out extensive simulations using results from the sensitivity analysis. These simulations offer a glimpse into the practical implications of our findings, bridging the gap between theoretical insights and practical applications. We discuss and summarize our findings in Section 6.

2. Model Formulation

To formulate the ticks-prey-predator dynamics with disease, we adapt some of the approaches used in earlier modeling of ticks dynamics in [24–26]. We assume that transovarial transmission is very unlikely for ehrlichiosis, so all eggs laid are without infection. The eggs hatch into susceptible larvae (L_S) which progresses into infectious larvae (L_I) after acquiring infection from feeding on an infected prey (M_I) at the rate λ_{LM} expressed as

$$\lambda_{LM} = \frac{\beta_{LM} M_I}{M},$$

where β_{LM} is the effective transmission probability and M is the total prey population (susceptible and infected). The susceptible and infected larvae mature at the rate σ_L or die in a density dependent manner ($\mu_L(L_S, L_I, M)$) express as

$$\mu_L(L_S, L_I, M) = 0.25 + \left[0.015 \ln\left(\frac{1.01 + L_S + L_I}{M}\right)\right].$$

Thus, we have the following equations for susceptible and infected larvae:

$$\begin{aligned} \frac{dL_S}{dt} &= \sigma_E E - \lambda_{LM} L_S - \sigma_L L_S - \mu_L(L_S, L_I, M) L_S, \\ \frac{dL_I}{dt} &= \lambda_{LM} L_S - \sigma_L L_I - \mu_L(L_S, L_I, M) L_I, \end{aligned}$$

Regardless of whether or not larvae are susceptible or infectious (L_S and L_I, respectively), they molt into nymphs at the rate σ_L once fully engorged from a blood meal, or die at the density dependent rate, $\mu_N(N_S, N_I, M, P)$ given as

$$\mu_N(N_S, N_I, M, P) = 0.45 + \left[0.02 \ln\left(\frac{1.01 + N_S + N_I}{M + P}\right)\right],$$

The nymph life-stage is the least discriminant when it comes to host preference and as such, we incorporate the potential for nymphs to feed on both prey and predator which are small and large hosts respectively. At this stage the susceptible nymphs may become infected if feeding on an infectious host. The force of infection, λ_{NM}, is defined as:

$$\lambda_{NM} = \frac{\beta_{NM} M_I}{M} + \frac{\beta_{NP} P_I}{P},$$

where β_{NM} is the probability that a susceptible nymph becomes infected after feeding on an infectious host. M, and P are the number of susceptible and infectious prey and predator hosts. The susceptible and infectious nymphs mature to become adult ticks at the rates σ_N. The equations describing the rates of change for susceptible and infectious nymph populations (N_S and N_I, respectively) are:

$$\begin{aligned}
\frac{dN_S}{dt} &= \sigma_L L_S - \lambda_{NM} N_S - \sigma_N N_S - \mu_N(N_S, N_I, M, P) N_S, \\
\frac{dN_I}{dt} &= \sigma_L L_I + \lambda_{NM} N_S - \sigma_N N_I - \mu_N(N_S, N_I, M, P) N_I,
\end{aligned}$$

The susceptible and infectious adult ticks quest for hosts, especially larger hosts like the predator population. At this point, there is the possibility of a susceptible tick becoming infected if feeding on an infectious host. The force of infection for feeding adult ticks is:

$$\lambda_{AP} = \frac{\beta_{AP} P_I}{P},$$

where β_{AP} is the probability that a susceptible adult becomes infected after feeding on an infectious host. The susceptible and infectious populations are reduced by natural death at the rates $(\mu_A(A_S, A_I, P)A_S)$, expressed as

$$\mu_A(A_S, A_I, P) = 0.35 + \left[0.03 \ln\left(\frac{1.01 + A_S + A_I}{P}\right)\right].$$

With these, we have the following equations for susceptible and infectious feeding adults, given as A_S and A_I:

$$\begin{aligned}
\frac{dA_S}{dt} &= \sigma_N N_S - \lambda_{AP} A_S - \mu_A(A_S, A_I, P) A_S, \\
\frac{dA_I}{dt} &= \sigma_N N_I + \lambda_{AP} A_S - \mu_A(A_S, A_I, P) A_I,
\end{aligned}$$

Note that once a larvae (or nymph or adult) becomes infectious, it remains so for the rest of its life.

Like the expression for the susceptible and infected tick populations we can express the susceptible and infected in the prey and predator systems as

$$\begin{aligned}
\frac{dM_S}{dt} &= \left(\frac{\pi_M}{1+\tau P}\right)\left(1-\frac{M}{K_M}\right)M - \left(\frac{\alpha_M P}{a+M}\right)M_S - \lambda_{MT}M_S - \mu_M M_S,\\
\frac{dM_I}{dt} &= \lambda_{MT}M_S - \mu_M M_I - \left(\frac{\alpha_M P}{a+M}\right)M_I,\\
\frac{dP_S}{dt} &= \frac{\pi_P(M_S+M_I)(P_S+P_I)}{a+M} - \lambda_{PA}P_S - \mu_P P_S,\\
\frac{dP_I}{dt} &= \lambda_{PA}P_S - \mu_P P_I,
\end{aligned}$$

where the forces of infection for the prey and predator λ_{MT} and λ_{PA} are express as:

$$\lambda_{MT} = \frac{\beta_{MT}(L_I+N_I)}{M}, \quad \lambda_{PA} = \frac{\beta_{PA}(N_I+A_I)}{P},$$

where β_{MT} and β_{PA} are the probability that a susceptible prey and predator becomes infected after been fed on by an infectious tick.

Furthermore, we assume that the host do not recover from the infection, see [27, 28]. With these assumptions we have the following system of equations for the eggs and the larvae, nymphs, and adults:

$$\begin{aligned}
\frac{dE}{dt} &= f\pi_E(A,P)\left(1-\frac{E}{K_E}\right)(A_S+A_I) - \sigma_E E - \mu_E E, \qquad (2.1)\\
\frac{dL_S}{dt} &= \sigma_E E - \lambda_{LM}L_S - \sigma_L L_S - \mu_L(L_S,L_I,M)L_S,\\
\frac{dL_I}{dt} &= \lambda_{LM}L_S - \sigma_L L_I - \mu_L(L_S,L_I,M)L_I,\\
\frac{dN_S}{dt} &= \sigma_L L_S - \lambda_{NM}N_S - \sigma_N N_S - \mu_N(N_S,N_I,M,P)N_S,\\
\frac{dN_I}{dt} &= \sigma_L L_I + \lambda_{NM}N_S - \sigma_N N_I - \mu_N(N_S,N_I,M,P)N_I,\\
\frac{dA_S}{dt} &= \sigma_N N_S - \lambda_{AP}A_S - \mu_A(A_S,A_I,P)A_S,\\
\frac{dA_I}{dt} &= \sigma_N N_I + \lambda_{AP}A_S - \mu_A(A_S,A_I,P)A_I,\\
\frac{dM_S}{dt} &= \left(\frac{\pi_M}{1+\tau P}\right)\left(1-\frac{M}{K_M}\right)M - \lambda_{MT}M_S - \left(\frac{\alpha_M P}{a+M}\right)M_S - \mu_M M_S,\\
\frac{dM_I}{dt} &= \lambda_{MT}M_S - \mu_M M_I - \left(\frac{\alpha_M P}{a+M}\right)M_I,\\
\frac{dP_S}{dt} &= \pi_P\left(\frac{M_S+M_I}{a+M}\right)(P_S+P_I) - \lambda_{PA}P_S - \mu_P P_S,\\
\frac{dP_I}{dt} &= \lambda_{PA}P_S - \mu_P P_I,
\end{aligned}$$

The model flow diagram is given in Figure 1.

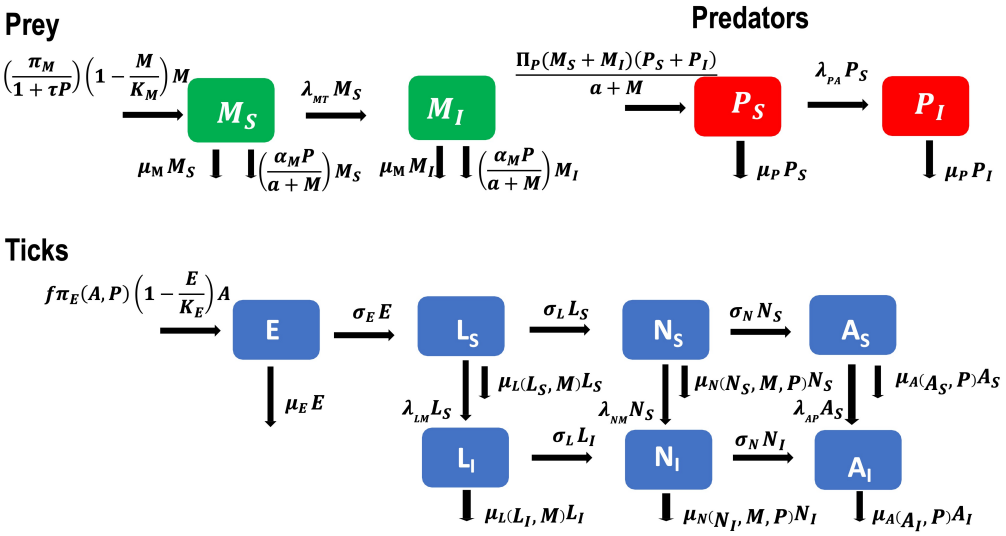

Figure 1. Flow diagram of ticks-prey-predator model (2.1) with disease.

2.1. Analysis of the ticks-prey-predator model (2.1)

2.1.1. Positivity and boundedness of solutions

Following the results in subsection 3.1 and the approach in Guo and Agusto [29] we can prove the following lemmas for model positivity and boundedness of solutions.

Lemma 1. *Let the initial data* $F(0) \geq 0$, *where* $F(t) = (E(t), L_S(t), L_I(t), N_S(t), N_I(t), A_S(t), A_I(t), M_S(t), M_I(t), P_S(t), P_I(t))$. *Then the solutions* $F(t)$ *of the system are non-negative for all* $t > 0$.

Lemma 2. *The region* $\Omega = \Omega_T \cup \Omega_{MP} \subset \mathbb{R}^7_+ \times \mathbb{R}^4_+$ *is positively-invariant for the system with non-negative initial conditions in* $\mathbb{R}^{11}_+$.
where,

$$\begin{aligned} \Omega_T &= \left\{(E(t), L_S(t), L_I(t), N_S(t), N_I(t), A_S(t), A_I(t)) \in \mathbb{R}^7_+ : \ E(t) \leq K_E, \ N_T(t) \leq \frac{\sigma_E K_E}{\mu_T}\right\}, \\ with, \mu_T &= min(\mu_L(L_S, L_I, M), \mu_N(N_S, N_I, M, P), \mu_A(A_S, A_I, P)), \end{aligned}$$

$N_T = L_S(t) + L_I(t) + N_S(t) + N_I(t) + A_S(t) + A_I$, *and* $E(t) < K_E$.

$$\Omega_{MP} = \left\{(M_S(t), M_I(t), P_S(t), P_I(t)) \in \mathbb{R}^4_+ \ : \ (M_S(t), M_I(t), P_S(t), P_I(t)) \leq \frac{r}{\eta}\right\},$$

where $r = \dfrac{K_M(\pi_M - \mu_M + \eta)^2}{4\pi_M} > 0.$

Proof. The first seven equations of model (2.1) give the following after summing the equations representing the larvae, nymphs, and adult stages

$$\frac{dE(t)}{dt} = f\pi_E(A,P)\left(1-\frac{E}{K_E}\right)(A_S+A_I)-(\sigma_E+\mu_E)E \tag{2.2}$$

$$\frac{dN_T(t)}{dt} = \sigma_E E-\mu_T N_T, \tag{2.3}$$

where $\mu_T = \min\{\mu_L(L_S,L_I,M),\mu_N(N_S,N_I,M,P),\mu_A(A_S,A_I,P)\}$, Since K_E is the carrying capacity, it follows that $E \le K_E$. Hence, equation (2.3) becomes

$$\frac{dN_T(t)}{dt} \le \sigma_E K_E-\mu_T N_T,$$

Thus,

$$N_T(t) \le \frac{\sigma_E K_E}{\mu_T}+\left(N_T(0)-\frac{\sigma_E K_E}{\mu_T}\right)e^{-\mu_T t}, \tag{2.4}$$

If $N_T(0) = \frac{\sigma_E K_E}{\mu_T}$, then $N_T(t) = \frac{\sigma_E K_E}{\mu_T}$. Hence, equation (2.4) implies that $N_T(t)$ is bounded. Furthermore, in Section 3.1 below, we show that the domain Ω_{MP} is bounded. Thus, all solutions starting in the region Ω remain in Ω. Hence, the region is positively-invariant and hence, the region Ω attracts all solutions in $\mathbb{R}^{11}_+$. □

2.1.2. Stability of disease-free equilibrium (DFE)

The tick-prey-predator model has a disease-free equilibrium (DFE) denoted by $\mathcal{E}_0$. The DFE is obtained by setting the right-hand sides of the equations in the model (2.1) to zero, which is given by

$$\mathcal{E}_0 = (E^*, L_S^*, 0, N_S^*, 0, A_S^*, 0, M_S^*, 0, P_S^*, 0),$$

The analytical expression of the DFE is difficult to obtain due to the nonlinearity of the density-dependent fecundity and mortality functions in the tick population, see subseection 3.1.2 above. To establish the stability of disease-free equilibrium ($\mathcal{E}_0$) we use the reproduction number $\mathcal{R}_0$ which is obtained using the next generation operator method on system (2.1). Taking L_I, N_I, A_I, M_I, and P_I as the infected compartments and then using the notation in [30], the Jacobian F and V matrices for new infectious terms and the remaining transfer terms are defined as:

$$F = \begin{pmatrix} 0 & 0 & 0 & 0 & \beta_{PA} \\ 0 & 0 & \beta_{MT} & \beta_{MT} & 0 \\ 0 & \frac{\beta_{LM}L_S^*}{M_S^*} & 0 & 0 & 0 \\ \frac{\beta_{NP}N_S^*}{P_S^*} & \frac{\beta_{NM}N_S^*}{M_S^*} & 0 & 0 & 0 \\ \frac{\beta_{AP}A_S^*}{P_S^*} & \frac{\beta_{AP}A_S^*}{P_S^*} & 0 & 0 & 0 \end{pmatrix}, \quad V = \begin{pmatrix} \mu_P & 0 & 0 & 0 & 0 \\ 0 & k_1 & 0 & 0 & 0 \\ 0 & 0 & k_2 & 0 & 0 \\ 0 & 0 & -\sigma_L & k_3 & 0 \\ 0 & 0 & 0 & -\sigma_N & \mu_{A_I}(P^*) \end{pmatrix},$$

where $k_1 = \dfrac{\alpha_M P^*}{a + M^*} + \mu_M$, $k_2 = \sigma_L + 0.25 + 0.015 \ln\left(\dfrac{1.01}{M_S^*}\right)$, $k_3 = \sigma_N + 0.45 + 0.02 \ln\left(\dfrac{1.01}{M_S^* + P_S^*}\right)$, and $\mu_{A_I}(P^*) = 0.35 + 0.03 \ln\left(\dfrac{1.01}{P_S^*}\right)$.

Therefore, the reproduction is given as $\mathcal{R}_0 = \rho(FV^{-1})$, where ρ is the spectra radius is given as

$$
\begin{aligned}
\mathcal{R}_0 \;=\; & \frac{\sqrt{2}}{2M_S^*\mu_{A_I}(P^*)P_S^*k_1k_2k_3\mu_p} \times \Big\{ M_S^*\mu_{A_I}(P^*)P_S^*k_1k_2k_3\mu_p \\
& \times \Big[k_1k_2\beta_{PA}(A_S^*k_3\beta_{AP} + N_S\beta_{NP}\sigma_N)M_S^* \\
& + \mu_{A_I}(P^*)\beta_{MT}\mu_p(L_S^*k_3\beta_{LM} + L_S^*\beta_{LM}\sigma_L + N_S^*k_2\beta_{NM})P_S^* \\
& + \Big([k_1k_2\beta_{PA}(A_S^*k_3\beta_{AP} + N_S\beta_{NP}\sigma_N)M_S^*]^2 \\
& - 2k_1k_2\beta_{PA}\mu_{A_I}(P^*)\beta_{MT}\mu_p[A_S^*k_3\beta_{AP}(L_Sk_3\beta_{LM} + L_S^*\beta_{LM}\sigma_L + N_S^*k_2\beta_{NM}) \\
& + N_S^*\beta_{NP}\sigma_N(L_S^*k_3\beta_{LM} - L_S^*\beta_{LM}\sigma_L - N_S^*k_2\beta_{NM})]M_S^*P_S^* \\
& + [\mu_{A_I}(P^*)\beta_{MT}\mu_p(L_S^*k_3\beta_{LM} + L_S^*\beta_{LM}\sigma_L + N_S^*k_2\beta_{NM})P_S^*]^2 \\
& + 4A_S^*(M_S^*)^2N_S^*\mu_{A_I}(P^*)k_1k_2^2k_3\beta_{AP}\beta_{MT}\beta_{NP}\beta_{PA}\mu_p \Big)^{\frac{1}{2}} \Big] \Big\}^{\frac{1}{2}},
\end{aligned}
$$

It is worth mentioning that $\mathcal{R}_0 > 0$ provided

$$
\begin{aligned}
& [k_1k_2\beta_{PA}(A_S^*k_3\beta_{AP} + N_S\beta_{NP}\sigma_N)M_S^*]^2 + [\mu_{aI}(aI,p)\beta_{MT}\mu_p(L_S^*k_3\beta_{LM} + L_S^*\beta_{LM}\sigma_L + N_S^*k_2\beta_{NM})P_S^*]^2 \\
& + 4A_S^*(M_S^*)^2N_S^*\mu_{aI}(aI,p)k_1k_2^2k_3\beta_{AP}\beta_{MT}\beta_{NP}\beta_{PA}\mu_p \\
& > 2k_1k_2\beta_{PA}\mu_{aI}(aI,p)\beta_{MT}\mu_p[A_S^*k_3\beta_{AP}(L_Sk_3\beta_{LM} + L_S^*\beta_{LM}\sigma_L + N_S^*k_2\beta_{NM}) \\
& + N_S^*\beta_{NP}\sigma_N(L_S^*k_3\beta_{LM} - L_S^*\beta_{LM}\sigma_L - N_S^*k_2\beta_{NM})]M_S^*P_S^*,
\end{aligned}
$$

Thus, the following result is established using Theorem 2 in [30].

Lemma 3. *The DFE of ticks-prey-predator model* (2.1) *with disease, given by $\mathcal{E}_0$, is locally asymptotically stable (LAS) if $\mathcal{R}_0 < 1$, and unstable if $\mathcal{R}_0 > 1$.*

The basic reproduction number ($\mathcal{R}_0$) measures the average number of new infections generated by a single infected individual (tick, prey or predator) in a completely susceptible population [30–33]. Thus, Lemma 3 implies that malaria can be eliminated from the human population (when $\mathcal{R}_0 < 1$) if the initial sizes of the sub-populations are in the basin of attraction of the DFE, $\mathcal{E}_0$.

3. Ticks-prey-predator model without disease

To formulate the ticks-prey-predator dynamics, we classified the *Amblyomma Americanum* ticks into the following life stages: egg E, larvae L, nymph N, and adult A while P and M are predator and prey populations respectively.

The number of eggs are determined, in part, by the number of egg-laying adults. The fecundity of egg-laying adults is reduced in a density-dependent manner by the factor $\pi_E(A, P)$, with a female having the capacity to lay a maximum of $f = 6000$ eggs if $\pi_E(A, P) = 1$. The function is given as:

$$\pi_E(A,P) \quad = \quad 1-\left\{0.25+\left[0.045\ln\left(\frac{1.01+A}{P}\right)\right]\right\},$$

where P is the population of the predator. The egg hatch into larvae at the rate σ_E or the decay at a fixed daily, per-capita rate (μ_E). The equation for the eggs (E) is given by:

$$\frac{dE}{dt} \quad = \quad f\pi_E(A,P)\left(1-\frac{E}{K_E}\right)A-(\sigma_E+\mu_E)E,$$

The larvae population (L) increases depending on the egg developmental rate or hatching rate (σ_E). The population decreases via maturation by a fixed rate σ_L as well as via death in a density dependent manner described as:

$$\mu_L(L,M)=0.25+\left[0.0155\ln\left(\frac{1.01+L}{M}\right)\right],$$

Thus, the equation for the larvae (L) population is given by:

$$\frac{dL}{dt} \quad = \quad \sigma_E E-[\sigma_L+\mu_L(L,M)]L,$$

The population of the nymphs increase following the maturation of the larvae. Nymphs that survive feeding on a host then become engorged, once engorged, they either molt into adult ticks at the rate σ_N, or die in a density-dependent manner described as:

$$\mu_N(N,M,P)=0.45+\left[0.025\ln\left(\frac{1.01+N}{M+P}\right)\right],$$

where M is population of the prey. Hence, the equations describing the rates of change for the nymph population (N) is given as:

$$\frac{dN}{dt} \quad = \quad \sigma_L L-[\sigma_N+\mu_N(N,M,P)]N,$$

Once attached to a host, the adult ticks can take up to several days to finish feeding. They may also die in a density dependent manner:

$$\mu_A(A,P)=0.35+\left[0.035\ln\left(\frac{1.01+A}{P}\right)\right],$$

All of these components lead to the following equations for adult ticks, given as:

$$\frac{dA}{dt} \quad = \quad \sigma_N N-\mu_A(A,P)A,$$

We assume that the prey population grew logistically; however, the population is also limited due to the fear of the predator at the rate $\left(\frac{\pi_M}{1+\tau P}\right)$, where π_M is the preys birth rate and τ regulates the strength of fear incited by the predator. This decreasing fear function $\left(\frac{1}{1+\tau P}\right)$ was first introduced by Wang et al. [20]. The function has gained widespread acceptance within the research community, as evidenced by its adoption and application in various studies. For more information, see [21,34,35] and references therein. Biologically meaningful properties are embedded within the fear function, which dictate its behavior within the model framework.

(i) In the absence of fear ($\tau = 0$), the fear function yields:

$$\frac{1}{1+0\cdot P} = 1,$$

(ii) When there are no predators ($P = 0$), the fear function becomes:

$$\frac{1}{1+\tau\cdot 0} = 1,$$

(iii) As the fear level increases ($\tau \to \infty$), the fear function approaches zero:

$$\lim_{\tau\to\infty} \frac{1}{1+\tau P} = 0,$$

(iv) When the predator population is abundant ($P \to \infty$), the fear function tends to zero, causing the birthrate or disease transmission rate to decline:

$$\lim_{P\to\infty} \frac{1}{1+\tau P} = 0,$$

The properties of the fear function represent biological and epidemiological factors such as fear intensity, predator presence, and population dynamics, all of which impact disease transmission.

The prey population is reduced by predation by a Holling type 2 functional response at the rate $\left(\frac{\alpha_M M}{a+M}\right)$, where α_M is the attack rate of the predator. We note that μ_M represents the death rate of the prey that is not influenced by fear of predators and thus is isolated from the logistic equation for the prey population. This novel phenomenon of splitting the natural death rate into two in prey dynamics involving fear of predation was recently introduced by Antwi-Fordjour et al. [36]. Thus, the rate of change of the prey population is expressed as:

$$\frac{dM}{dt} = \left(\frac{\pi_M}{1+\tau P}\right)\left(1-\frac{M}{K_M}\right)M - \left(\frac{\alpha_M P}{a+M}\right)M - \mu_M M,$$

The predator population increases after predation of the prey population at the rate $\left(\frac{\pi_P M}{a+M}\right)$, where π_P is the energy conversion rate due to predation of the prey. The energy conversion rate from prey to predator measures how efficiently a predator converts the energy from its prey into its own growth and reproduction. The predator population is reduced due to mortality at the rate μ_P. Thus the equation of the predator population is given as:

$$\frac{dP}{dt} = \left(\frac{\pi_P M}{a+M}\right)P - \mu_P P,$$

Combining the above description and assumptions we have the following system of equations for the ticks-prey-predator system:

$$\begin{aligned}
\frac{dE}{dt} &= f\pi_E(A,P)\left(1-\frac{E}{K_E}\right)A - (\sigma_E+\mu_E)E \\
\frac{dL}{dt} &= \sigma_E E - \sigma_L L - \mu_L(L,M)L \\
\frac{dN}{dt} &= \sigma_L L - \sigma_N N - \mu_N(M,N,P)N \\
\frac{dA}{dt} &= \sigma_N N - \mu_A(A,P)A \\
\frac{dM}{dt} &= \left(\frac{\pi_M}{1+\tau P}\right)\left(1-\frac{M}{K_M}\right)M - \left(\frac{\alpha_M P}{a+M}\right)M - \mu_M M \\
\frac{dP}{dt} &= \left(\frac{\pi_P M}{a+M}\right)P - \mu_P P,
\end{aligned} \tag{3.1}$$

The model flow diagram is given in Figure 2 and the description of the parameters and the values used in simulations are given in Table 1.

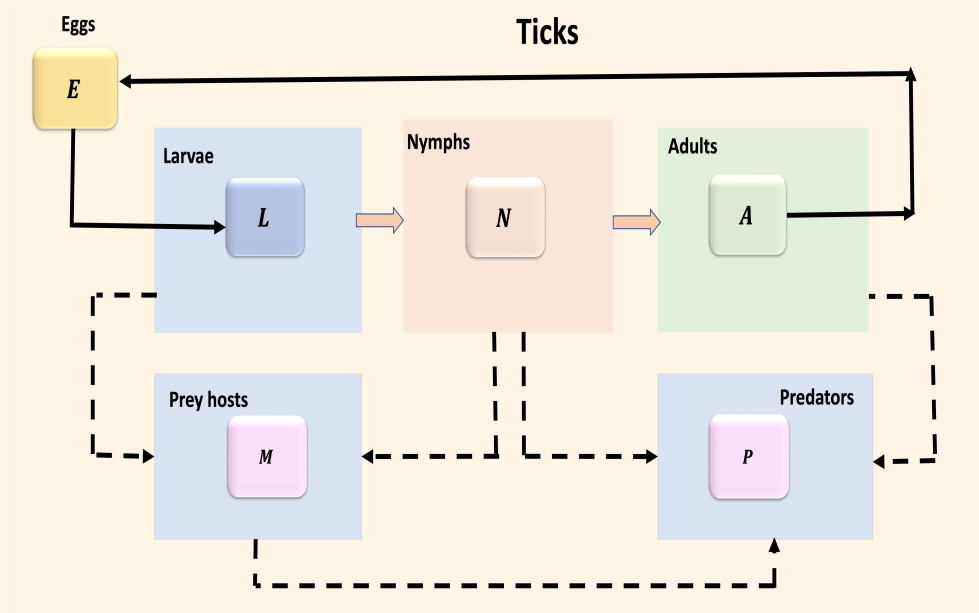

Figure 2. Flow diagram of ticks-prey-predator model (3.1) .

Table 1. Description of the parameters of the ticks-prey-predator model (3.1). Tick related parameter values and estimates are taken from [24, 25] and the varied prey-predator related parameter values are biologically feasible.

Parameter/Variable	Description	Value	References
π_E	Growth rate of eggs dependent on A and P		[24, 25]
μ_L	Larva death rate as a function of L and M		[24, 25]
μ_N	Nymphs death rate as a function of M, N and P		[24, 25]
μ_A	Adults ticks death rate as a function of A and P		[24, 25]
f	Birthrate of tick eggs	6000	[25]
K_E	Carrying capacity of eggs	15000	Variable
σ_E	Eggs maturation rate	1/5	[25]
μ_E	Eggs in-viability rate	0.008	[25]
σ_L	Larva maturation rate	1/5	[25]
σ_N	Nymphs maturation rate	1/7	[25]
π_M	Preys birth rate	0.8	Variable
τ	Strength of fear of predators	1	[37]
K_M	Carrying capacity of preys	1	[38]
μ_M	Preys natural death rate	0.1	[39]
α_M	Predators attack rate	0.5	[39]
a	Half saturation constant	0.4	Variable
π_P	Predator biomass conversion efficiency	1.5	Variable
μ_P	Predators natural death rate	0.3	Variable

3.1. Quantitative analysis of ticks-prey-predator model (3.1)

3.1.1. Positivity and boundedness of solutions

We shall investigate the positivity and boundedness of the prey and predator populations of system (3.1). From an ecological standpoint, the biomass of a population cannot exhibit negativity at any point in time, thereby necessitating the persistence of non-negative solutions. Boundedness guarantees that these populations will not undergo exponential growth over an extended duration.

Theorem 1. *For all $t \geq 0$, the solutions $(M(t), P(t))$ of the system* (3.1) *with initial conditions $M(0) \geq 0$ and $P(0) \geq 0$ remain non-negative.*

Proof. Since the functions on the right-hand side of system (3.1) are continuous and locally Lipschitz in the positive octant $\mathbb{R}^2_+$, the system has a unique solution that exists for all $t \in [0, \infty)$.

The predator (P) and prey (M) equations of system (3.1) can be rewritten as

$$\begin{aligned} \frac{dM}{dt} &= Mg_1(M, P) \\ \frac{dP}{dt} &= Pg_2(M, P), \end{aligned} \tag{3.2}$$

where

$$g_1(M,P) = \left(\frac{\pi_M}{1+\tau P}\right)\left(1-\frac{M}{K_M}\right) - \left(\frac{\alpha_M P}{a+M}\right) - \mu_M$$
$$g_2(M,P) = \left(\frac{\pi_P M}{a+M}\right) - \mu_P,$$

We apply the integrating factor technique to system (3.2), a fundamental method for solving differential equations, to find the solutions of the system (3.1);

$$M(t) = M(0)\exp\left(\int_0^t g_1(M,P)\,ds\right),$$
$$P(t) = P(0)\exp\left(\int_0^t g_2(M,P)\,ds\right),$$

From the expressions above, it is clear that $M(t)$ and $P(t)$ remain non-negative for all future time if they initiate from an interior initial point of

$$\mathbb{R}^2_+ = \{(M(t),P(t)) : M(t) \geq 0, P(t) \geq 0\},$$

□

Theorem 2. *The solutions* $(M(t),P(t))$ *of system* (3.1) *with initial conditions* $M(0) > 0, P(0) > 0$ *are ultimately bounded.*

Proof. Consider the function $W(M(t),P(t)) = M(t) + P(t)$. Thus

$$\begin{aligned}\frac{dW(M(t),P(t))}{dt} &= \frac{dM}{dt} + \frac{dP}{dt}\\ &= \left(\frac{\pi_M}{1+\tau P}\right)\left(1-\frac{M}{K_M}\right)M - \left(\frac{\alpha_M P}{a+M}\right)M - \mu_M M + \left(\frac{\pi_P P}{a+M}\right)M - \mu_P P\\ &= \left(\frac{\pi_M}{1+\tau P}\right)\left(1-\frac{M}{K_M}\right)M + \left(\frac{(\pi_P-\alpha_M)P}{a+M}\right)M - \mu_M M - \mu_P P,\end{aligned}$$

Assume $\pi_P < \alpha_M$, and $\eta \in \mathbb{R}_+$ such that $\eta \leq \mu_P$ and $\pi_M + \eta > \mu_M$. Due to the positivity of the solutions, it is obvious that $M(t) \leq K_M$ by comparison to the logistic equation.

Then,

$$\begin{aligned}\frac{dW}{dt} + \eta W &= \left(\frac{\pi_M}{1+\tau P}\right)\left(1-\frac{M}{K_M}\right)M + \left(\frac{(\pi_P-\alpha_M)P}{a+M}\right)M - \mu_M M - \mu_P P + \eta(M+P)\\ &\leq \left(\frac{\pi_M}{1+\tau P}\right)\left(1-\frac{M}{K_M}\right)M - \mu_M M - \mu_P P + \eta(M+P)\\ &\leq \pi_M\left(1-\frac{M}{K_M}\right)M - \mu_M M - \mu_P P + \eta(M+P)\\ &= \pi_M M - \frac{\pi_M}{K_M}M^2 - \mu_M M - \mu_P P + \eta M + \eta P\end{aligned}$$

$$
\begin{aligned}
&= (\pi_M - \mu_M + \eta)M - \frac{\pi_M}{K_M}M^2 - (\mu_P - \eta)P \\
&\leq (\pi_M - \mu_M + \eta)M - \frac{\pi_M}{K_M}M^2 \\
&\leq \frac{K_M(\pi_M - \mu_M + \eta)^2}{4\pi_M} = r,
\end{aligned}
$$

where $r = \dfrac{K_M(\pi_M - \mu_M + \eta)^2}{4\pi_M} > 0$. By solving the differential inequality above, we obtain the solution

$$0 \leq W(M(t), P(t)) \leq \frac{r}{\eta}(1 - e^{-\eta t}) + W(M(0), P(0))e^{-\eta t},$$

Thus,

$$0 \leq W(M(t), P(t)) \leq \frac{r}{\eta}, \quad as \quad t \to \infty,$$

Therefore, the solutions $(M(t), P(t))$ to the system (3.1) with positive initial conditions are ultimately bounded. □

3.1.2. Stability analysis of the equilibrium points

To find equilibrium points, we need to set the derivatives of all variables to zero and solve the resulting equations simultaneously.

$$
\begin{aligned}
f\pi_E(P)\left(1 - \frac{E}{K_E}\right)A - \sigma_E E - \mu_E E &= 0 \\
\sigma_E E - \sigma_L L - \mu_L(M)L &= 0 \\
\sigma_L L - \sigma_N N - \mu_N(M, P)N &= 0 \\
\sigma_N N - \mu_A(P)A &= 0 \\
\left(\frac{\pi_M M}{1 + \tau P}\right)\left(1 - \frac{M}{K_M}\right) - \left(\frac{\alpha_M P}{a + M}\right)M - \mu_M M &= 0 \\
\left(\frac{\pi_P M}{a + M}\right)P - \mu_P P &= 0,
\end{aligned}
$$

Denote the equilibrium values as follows:

$$P = P^*, M = M^*, E = E^*, L = L^*, N = N^*, A = A^*$$

Since the equations are highly nonlinear in nature due to the density-dependent fecundity and mortality in the tick population, making it difficult to find analytical solutions. As a result, it may not be feasible to solve them explicitly. Instead, it may be necessary to employ numerical methods or utilize software tools to obtain approximate values for the equilibrium points.

However, it is biologically feasible to assume that the number of larvae, nymphs, and adult ticks are smaller than the number of eggs (that is, $A < N < L < K_E$), since most ticks die if they are unable

to find a host to fed on [40]; from subsection 3.1 above we have that the prey and predator population are bounded, that is $|M| \leq C_1$ and $|P| \leq C_2$, where C_1 and C_2 are non-negative constants; then we can assume that the tick fecundity and mortality are constant rates (that is $\pi_E,\ \mu_E,\ \mu_L,\ \mu_N$, and μ_A). Thus model (3.1) reduces to the following simple system

$$\begin{aligned} \frac{dT}{dt} &= \pi_T - \mu_T T \\ \frac{dM}{dt} &= \left(\frac{\pi_M M}{1+\tau P}\right)\left(1 - \frac{M}{K_M}\right) - \left(\frac{\alpha_M P}{a+M}\right)M - \mu_M M \\ \frac{dP}{dt} &= \left(\frac{\pi_P M}{a+M}\right)P - \mu_P P, \end{aligned} \tag{3.3}$$

where $\pi_T = f\pi_E$, and T denotes the total tick population from eggs to adult. The reduced system (3.3) has three non-negative steady states namely:

(i) Tick-only equilibrium $(T, M, P) = \left(\frac{\pi_T}{\mu_T}, 0, 0\right)$.

(ii) Predator-free equilibrium $(T, M, P) = \left(\frac{\pi_T}{\mu_T}, K_M\left(1 - \frac{\mu_M}{\pi_M}\right), 0\right)$ for $\pi_M > \mu_M$.

(iii) The coexistence equilibrium $(T^*, M^*, P^*) = \left(\frac{\pi_T}{\mu_T}, \frac{a\mu_P}{\pi_P - \mu_P}, \frac{-w_1 \mp \sqrt{w_2}}{2\alpha_M\sqrt{K_M}\tau(\pi_P - \mu_P)}\right)$, where $\pi_P > \mu_P,\ w_2 > w_1^2$, and

$$\begin{aligned} w_1 &= \sqrt{K_M}\left(a\mu_M\tau\pi_P + \alpha_M(\pi_P - \mu_P)\right), \\ w_2 &= K_M\left[(\alpha_1 - a\mu_M\tau)^2 + 4a\alpha_M\tau\pi_M\right]\pi_P^2 \\ &\quad - 2\alpha_M\mu_P\left[K_M(\alpha_M - a\mu_M\tau) + \alpha_M^2 K_M\mu_P^2 + 2a\tau\pi_M(a + K_M)\right]\pi_P, \end{aligned}$$

Thus, the following Theorem gives the conditions for the stability of equilibrium points obtained from system (3.3).

Theorem 3. *Consider the system given by system* (3.3)*. Then the following statements hold:*

(i) The tick-only equilibrium is locally asymptotically stable if $\mu_M > \pi_M$,

(ii) The predator-free equilibrium point is locally asymptotically stable if $\mu_P > \frac{K_M\pi_P(\mu_M - \pi_M)}{K_M\mu_M - \pi_M(a+K_M)}$,

(iii) The coexistence equilibrium is locally asymptotically stable provided the signs of w_3 and w_4 given in (3.6) *are positive.*

Proof. The Jacobain matrix for the system (3.3) at any equilibrium point is given as

$$J = \begin{pmatrix} -\mu_T & 0 & 0 \\ 0 & -\frac{a\alpha_M P}{(a+M)^2} + \frac{\pi_M(K_M - 2M)}{K_M(\tau P+1)} - \mu_M & \frac{\tau\pi_M M(M-K_M)}{K_M(\tau P+1)^2} - \frac{\alpha_M M}{a+M} \\ 0 & \frac{a\pi_P P}{(a+M)^2} & \frac{\pi_P M}{a+M} - \mu_P \end{pmatrix}, \tag{3.4}$$

(i) To analyze the stability of the equilibrium where only ticks are present, we begin by evaluating the Jacobian matrix at the tick-only equilibrium point.

$$J^* = \begin{pmatrix} -\mu_T & 0 & 0 \\ 0 & \pi_M - \mu_M & 0 \\ 0 & 0 & -\mu_P \end{pmatrix},$$

The eigenvalues associated with the Jacobian matrix J^* are $\lambda_1 = -\mu_T < 0$, $\lambda_2 = \pi_M - \mu_M$ and $\lambda_3 = -\mu_P < 0$. Thus the tick-only equilibrium is locally asymptotically stable if $\mu_M > \pi_M$.

(ii) To investigate the stability of predator-free equilibrium, we evaluate the Jacobian matrix at the predator-free equilibrium point,

$$J^{**} = \begin{pmatrix} -\mu_T & 0 & 0 \\ 0 & -\pi_M + \mu_M & \frac{K_M(\mu_M-\pi_M)\left(\pi_M\left(\mu_M\tau(a+K_M)+\alpha_M(P\tau+1)^2\right)-K_M\mu_M^2\tau\right)}{\pi_M(P\tau+1)^2(\pi_M(a+K_M)-K_M\mu_M)} \\ 0 & 0 & \frac{K_M\pi_P(\mu_M-\pi_M)}{K_M\mu_M-\pi_M(a+K_M)} - \mu_P \end{pmatrix}, \tag{3.5}$$

The eigenvalues associated with the Jacobian matrix J^{**} are $\lambda_1 = -\mu_T < 0$, $\lambda_2 = -\pi_M + \mu_M < 0$ and $\lambda_3 = \frac{K_M\pi_P(\mu_M-\pi_M)}{K_M\mu_M-\pi_M(a+K_M)} - \mu_P$. Thus the predator-free equilibrium is locally asymptotically stable if $\mu_P > \frac{K_M\pi_P(\mu_M-\pi_M)}{K_M\mu_M-\pi_M(a+K_M)}$,

(iii) From the Jacobian matrix (3.4), we derive the following characteristic equation

$$(-\mu_T - \lambda)\left(\lambda^2 + w_3\lambda + w_4\right) = 0, \tag{3.6}$$

where

$$w_3 = \frac{a\alpha_M P}{(a+M)^2} - \frac{\pi_P M}{a+M} + \frac{2\pi_M M}{K_M(\tau P+1)} + \mu_M + \mu_P - \frac{\pi_M}{\tau P+1},$$

note that $w_3 > 0$, if

$$\mu_M + \mu_P > \frac{\pi_P M}{a+M} + \frac{\pi_M}{\tau P+1} - \frac{a\alpha_M P}{(a+M)^2} - \frac{2\pi_M M}{K_M(\tau P+1)},$$

and

$$\begin{aligned} w_4 = &-\frac{2\pi_M\pi_P M^2}{K_M(a+M)(\tau P+1)} - \frac{a\tau\pi_M\pi_P M^2 P}{K_M(a+M)^2(\tau P+1)^2} - \frac{\mu_M\pi_P M}{a+M} + \frac{a\alpha_M\mu_P P}{(a+M)^2} \\ &+ \frac{\pi_M\pi_P M}{(a+M)(\tau P+1)} + \frac{a\tau\pi_M\pi_P MP}{(a+M)^2(\tau P+1)^2} + \frac{2\mu_P\pi_M M}{K_M(\tau P+1)} + \mu_M\mu_P - \frac{\mu_P\pi_M}{\tau P+1}, \end{aligned}$$

Additionally, $w_4 > 0$ if

$$\begin{aligned} \mu_M\mu_P > &\frac{2\pi_M\pi_P M^2}{K_M(a+M)(\tau P+1)} + \frac{a\tau\pi_M\pi_P M^2 P}{K_M(a+M)^2(\tau P+1)^2} + \frac{\mu_M\pi_P M}{a+M} - \frac{a\alpha_M\mu_P P}{(a+M)^2} \\ &- \frac{\pi_M\pi_P M}{(a+M)(\tau P+1)} - \frac{a\tau\pi_M\pi_P MP}{(a+M)^2(\tau P+1)^2} - \frac{2\mu_P\pi_M M}{K_M(\tau P+1)} + \frac{\mu_P\pi_M}{\tau P+1}, \end{aligned}$$

The eigenvalues associated with the equation in (3.6) are $\lambda_1 = -\mu_T < 0$ and other two roots (i.e., λ_2 and λ_3) of the quadratic equation in $\lambda^2 + w_3\lambda + w_4 = 0$. The other roots are given as $\lambda_2 + \lambda_3 = w_3 > 0$ and $\lambda_2\lambda_3 = w_4 > 0$. Thus the stability of the coexistence equilibrium point depend on sign of w_3 and w_4.

□

4. Sensitivity analysis for models (2.1) and (3.1)

Deterministic model outputs are governed by its input parameters, which exhibit some uncertainty in the process of their selection. Exploration of the ticks-prey-predator models (2.1) and (3.1) above requires determination of which parameters most strongly affect key model outputs (such as the number of infected individuals). A global sensitivity analysis was carried out using Latin Hypercube Sampling (LHS) and partial rank correlation coefficients (PRCC) to assess the impact of parameter uncertainty and the sensitivity of these key model outputs of the numerical simulations to variations in each parameter. LHS is a stratified sampling without replacement technique which allows for an efficient analysis of parameter variations across simultaneous uncertainty ranges in each parameter [41–44]. To generate the LHS matrices, we assume that all the model parameters are uniformly distributed. PRCC measures the strength of the relationship between the model outcome and the parameters, stating the degree of the effect that each parameter has on the outcome [41–44]. It is a reliable sensitivity measure for nonlinear yet monotonic relationships between the model input and output, provided that the inputs have minimal or no correlation [42].

We start by exploring first the sensitivity analysis of model(3.1) without disease and then model (2.1) with disease.

4.1. Sensitivity analysis of model (3.1) *without disease*

For the ticks-prey-predator model (3.1), a total of 1,000 runs were then carried out for the model using parameter values sampled from the LHS matrix and the outcome were ranked using the PRCC method. The parameter values used are given in Tables 1 (with ranges varying from ±20% the stated baseline values). The response functions in this case are the sum of the ticks $L + N + A$, the preys (M), and the predators (P).

The outcomes of the global sensitivity analysis are shown in Figure 3 and given in Table 2.

The parameters with the most significant impact on the sum of ticks ($L + N + A$) are tick eggs maturation rate (σ_E), the egg carrying capacity (K_E), the predator birth and natural death rates (π_P, and μ_P), the predator's attack rate (α_M), and the half saturation constant (a). Details are shown in Figure 3(a).

The significant parameters for prey (M) response function are shown in Figure 3(b); these parameters are the carrying capacity (K_M) of the prey, the predator birth and natural death rates (π_P, and μ_P), the predators attack rate (α_M), and the half saturation constant (a).

For the predators (P) response function, the significant parameters are the predators birth and natural death rate (π_P and μ_P). Other parameters are the preys' birth and natural death rate (π_M and μ_M) and their carrying capacity (K_M). The predators attack rate (α_M), the half saturation constant (a), and the fear of predators (τ) are equally significant, see Figure 3(c).

Note that the fear factor τ have a variable sensitivity indices for the three response function. It has a negative impact on the sum of the infected ticks, and the predator, and a positive significant impact on the prey population; however, the magnitude of the index is small.

The sensitivity indices are either positive or negative indicating the direction of the impact on the response functions, and the values of the indices indicate the magnitude of the response functions, see Table 2.

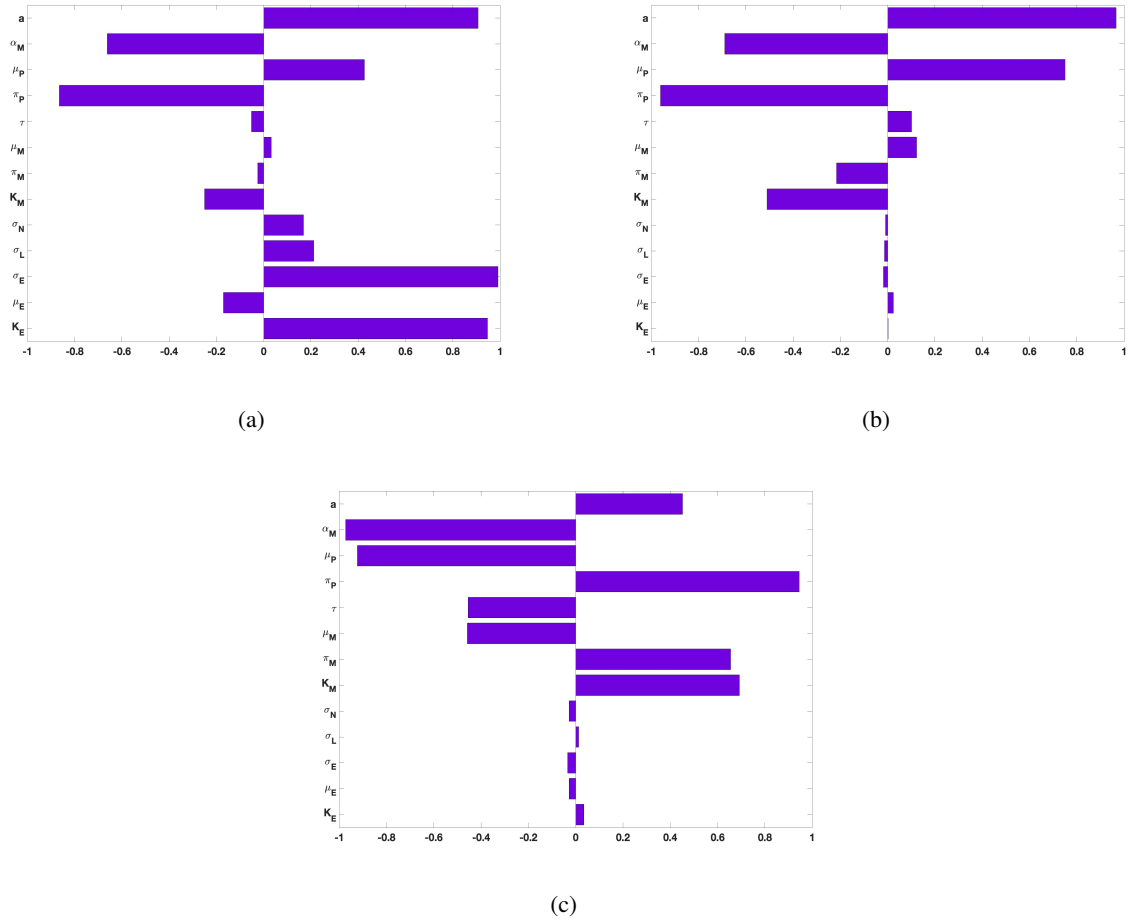

Figure 3. PRCC values for the ticks-prey-predator model (3.1) using as response functions (a) sum of ticks $L + N + A$; (b) prey (M); and (c) predator (P). Parameter values used are as given in Table 1.

4.2. Sensitivity analysis of model (2.1) *with disease*

For ticks-prey-predator model (2.1) a total of 1,000 simulations (runs) of the model for the LHS matrix were also carried out, using the parameter values given in Tables 1 (with ranges also varying from ±20% the stated baseline values) and the same response functions namely the sum of infected ticks $L_I + N_I + A_I$, infected preys (M_I), and infected predators (P_I). The PRCC method was then used to rank the parameter after the simulation runs were completed. The outcomes of the global sensitivity analysis are shown in Figure 4 and given in Table 3.

Figure 4(a) depict the parameters with the most significant impact on the sum of infected ticks ($L_I + N_I + A_I$), these are tick eggs maturation rate (σ_E), the egg carrying capacity (K_E), the predators birth rate (π_P), the predators attack rate (α_M), and the half saturation constant (a).

The impact of the model parameters on the infected preys (M_I) are shown in Figure 4(c). The impact of the parameters on the response function M_I are small, however, some of the effect of these parameters significant on M_I. The significant parameters are the nymphs maturation rate (σ_N), the

Table 2. PRCC and p-values of the ticks-prey-predator model (2.1) using the sum of ticks $L + N + A$, prey (M), and predator (P) as response functions.

Response function	$L+N+A$		M		P	
Parameters	PRCC	p-value	PRCC	p-value	PRCC	p-value
K_E	0.9471	0	0.0022	0.9439	0.0345	0.2784
μ_E	-0.1706	≤ 0.0001	0.0245	0.4423	-0.0277	0.3845
σ_E	0.9920	0	-0.0184	0.5642	-0.0337	0.2895
σ_L	0.2118	≤ 0.0001	-0.0137	0.6668	0.0130	0.6822
σ_N	0.1685	≤ 0.0001	-0.0091	0.7744	-0.0274	0.3888
K_M	-0.2504	≤ 0.0001	-0.5105	≤ 0.0001	0.6927	≤ 0.0001
π_M	-0.0250	0.4327	-0.2162	≤ 0.0001	0.6557	≤ 0.0001
μ_M	0.0326	0.3064	0.1229	0.0001	-0.4581	≤ 0.0001
τ	-0.0521	0.1019	0.1014	0.0014	-0.4550	≤ 0.0001
π_P	-0.8651	≤ 0.0001	-0.9615	0	0.9453	0
μ_P	0.4262	≤ 0.0001	0.7504	≤ 0.0001	-0.9239	0
α_M	-0.6624	≤ 0.0001	-0.6895	≤ 0.0001	-0.9727	0
a	0.9073	0	0.9671	0	0.4524	≤ 0.0001

predator birth rates (π_P), and the half saturation constant (a).

Lastly for the infected predators (P_I) depicted in Figure 4(c), the significant parameters are the egg carrying capacity (K_E), the probability that a susceptible prey becomes infected from an infectious larvae tick (β_{LM}), the prey carrying capacity (K_M), preys birth and natural death rate (π_M and μ_M). Other parameters are the fear of the predator (τ), predator biomass conversion efficiency (π_P), predators natural death rate (μ_P), the predators attack rate (α_M), and the half saturation constant (a).

The fear term τ as for model (3.1) have a variable sensitivity indices for the three response function. It has a negative impact on the sum of the infected ticks, and the predator, and a positive significant impact on the prey population; however, the magnitude of the index is small.

It is interesting to note that the infection transmission probabilities have mostly non-significant impact on all the response functions $L_I+N_I+A_I$, M_I, and P_I except for the probability that a susceptible prey becomes infected from an infectious larvae tick (β_{LM}).

Parameters with the largest partial rank correlation coefficient (PRCC) values have the largest impact on each of the response functions. The parameters with positive PRCC values have a positive impact on the response function and lead to increase in their values. While the parameters with negative PRCC values will reduce the response function values.

5. Numerical simulations

In this section, we simulate models (2.1) and (3.1) using initial conditions and parameter values that lead to unstable and stable dynamics, see Section 3.1. We start with the tick-prey-predator model (3.1) without disease and choose the unstable equilibrium due to the interesting dynamics exhibited by this equilibrium point. We also simulate the model (3.1) to show the impact of the attack rate and

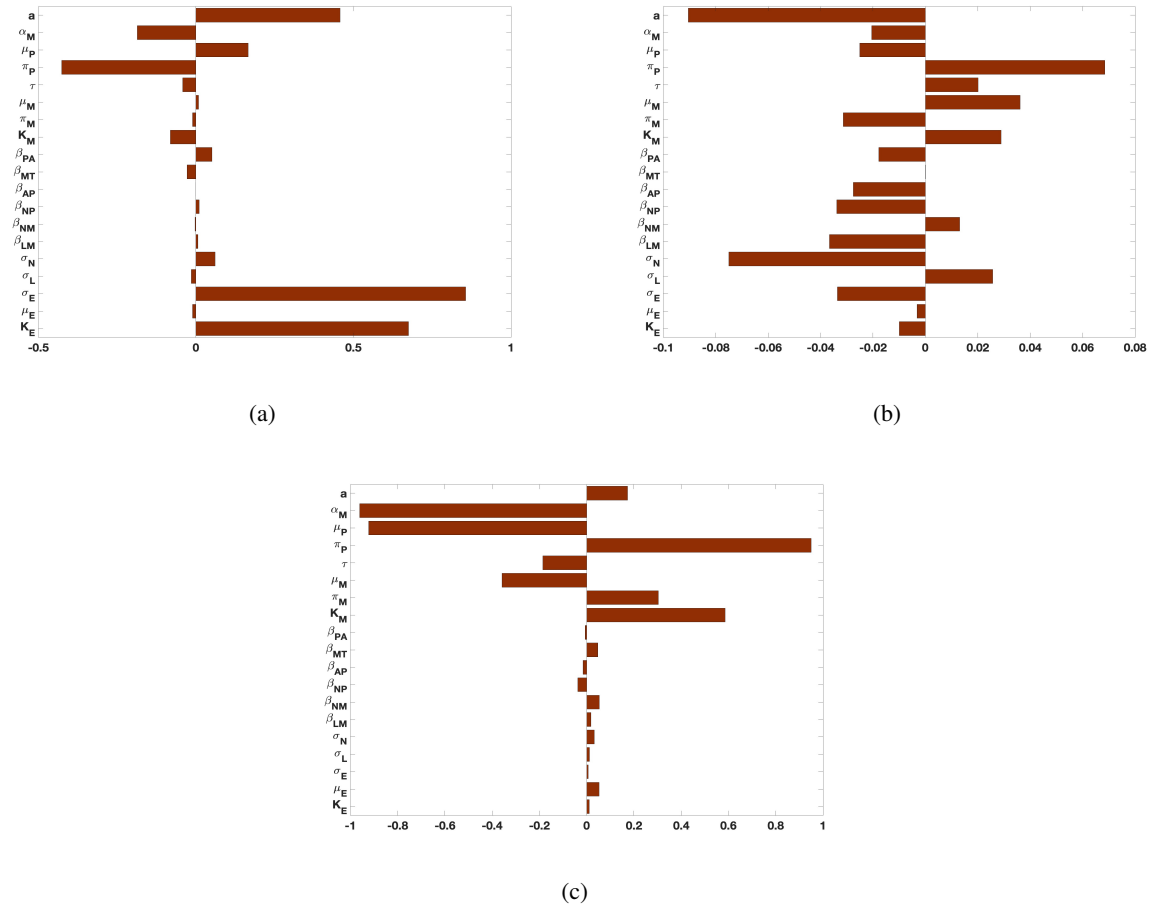

(a) (b)

(c)

Figure 4. PRCC values for the ticks-prey-predator model (2.1) using as response functions (a) sum of infected ticks $L_I + N_I + A_I$; (b) infected prey (M_I); and (c) infected predator (P_I). Parameter values used are as given in Table 1.

fear of the predator following the result of the sensitivity analysis in Section 4. Lastly, we simulate the ticks-prey-predator model (2.1) with disease to show the disease transmission dynamics given the interactions between the ticks, prey, and predator.

5.1. Numerical simulations of model (3.1)

5.1.1. Stable and unstable dynamics

We simulate the ticks-prey-predator model (3.1) using initial conditions and parameters values that lead to unstable and stable dynamics and focus on the prey-predator interaction. Figure 5(a) shows the dynamics when the equilibrium is unstable; while Figure 5(b) shows the dynamics when the equilibrium is stable. We see in Figure 5(a) an oscillatory dynamics as the prey and predator interact. This oscillatory behavior dissipates in a stable environment; see Figure 5(b). A stable attractor is observed in Figure 5(c). Here, the trajectory of the initial condition (IC) converges toward a stable limit cycle.

Next, we simulate the ticks-prey-predator model (3.1) for the unstable prey-predator equilibrium to

Table 3. PRCC and p-values of the ticks-prey-predator model (2.1) using the sum of infected ticks $L_I + N_I + A_I$, infected prey (M_I), and infected predator (P_I) as response functions.

Response function	$L_I + N_I + A_I$		M_I		P_I	
Parameters	PRCC	p-value	PRCC	p-value	PRCC	p-value
K_E	0.6749	≤ 0.0001	-0.0100	0.7546	0.0111	0.7280
μ_E	-0.0105	0.7436	-0.0032	0.9198	0.0528	0.0985
σ_E	0.8561	≤ 0.0001	-0.0335	0.2938	0.0070	0.8261
σ_L	-0.0144	0.6513	0.0257	0.4205	0.0116	0.7162
σ_N	0.0611	0.0557	-0.0750	0.0187	0.0323	0.3118
β_{LM}	0.0064	0.8411	-0.0366	0.2521	0.0183	0.5672
β_{NM}	-0.0031	0.9234	0.0131	0.6814	0.0535	0.0936
β_{NP}	0.0103	0.7474	-0.0338	0.2898	-0.0377	0.2384
β_{AP}	-0.0003	0.9929	-0.0275	0.3887	-0.0153	0.6321
β_{MT}	-0.0280	0.3810	-0.0001	0.9974	0.0476	0.1359
β_{PA}	0.0508	0.1113	-0.0177	0.5786	-0.0070	0.8263
K_M	-0.0812	0.0109	0.0289	0.3651	0.5860	≤ 0.0001
π_M	-0.0108	0.7359	-0.0313	0.3269	0.3033	≤ 0.0001
μ_M	0.0087	0.7849	0.0361	0.2579	-0.3583	≤ 0.0001
τ	-0.0421	0.1875	0.0201	0.5287	-0.1858	≤ 0.0001
π_P	-0.4257	≤ 0.0001	0.0685	0.0319	0.9502	0
μ_P	0.1660	≤ 0.0001	-0.0251	0.4327	-0.9229	0
α_M	-0.1864	≤ 0.0001	-0.0205	0.5213	-0.9606	0
a	0.4577	≤ 0.0001	-0.0905	0.0045	0.1729	≤ 0.0001

see the effect of the prey-predator interaction on the tick dynamics. Figure 6(a) shows the prey-predator interaction as in Figure 5. In Figure 6(b) we plot the simulation result of larvae and prey together. The figure shows the larvae population following the trajectory to the prey population. Similarly, we plot the simulation results of the eggs, nymphs, adults, along with predator. We also observed in Figure 6(c) the nymphs and the adult population following, in this case, the trajectory of the predator population, but that is not the case with the eggs.

5.2. Numerical simulations of model (2.1) *with disease*

We simulate the ticks-prey-predator model (2.1) with disease using initial conditions and parameters values that lead to unstable dynamics and show the disease transmission dynamics given the interactions between the ticks, prey, and predator. We observed oscillatory dynamics in susceptible and infected populations as prey and predator interact (see Figure 7). These oscillatory dynamics are similar to the dynamics observed in model (3.1) without disease. Figure 7(a) shows the dynamics among the susceptible ticks, and prey population while Figure 7(b) shows the dynamics of the infected ticks and the prey population.

We observed in Figure 7(a) the trajectory of the susceptible larvae population follow the trajectory of the susceptible prey population as the model without disease. While susceptible nymphs and adults follow the trajectories of susceptible predators, see Figure 7(c). For the infected larvae in Figure

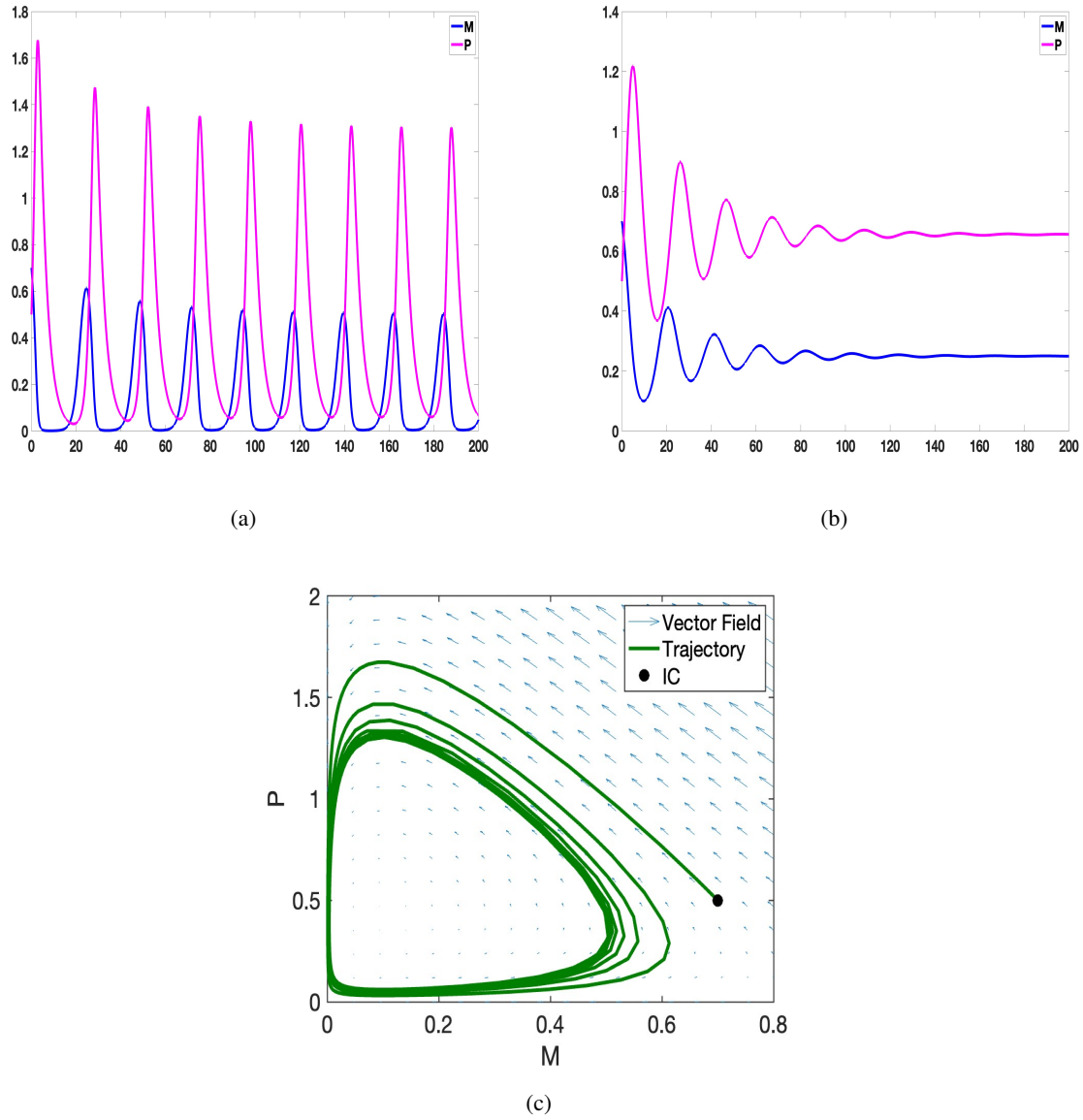

Figure 5. Numerical simulations of the ticks-prey-predator model (3.1) showing the prey-predator interaction when (a) the equilibrium is unstable; (b) the equilibrium is stable; (c) a stable limit cycle is observed from the phase portrait

7(b), we observed more infected larvae when the infected prey population are low and few infected larvae when there are more infected prey. We also observed in Figures 7(c) and 7(d) the trajectories of the nymphs and adult population either susceptible or infected follow the trajectory of the predator population (susceptible or infected).

5.2.1. Simulation scenario based on sensitivity analysis

Next, we run some simulation scenario using the results from the sensitivity analysis varying the prey-predator parameters α_M (predator attack rate), τ (strength of fear of predators). The parameter α_M

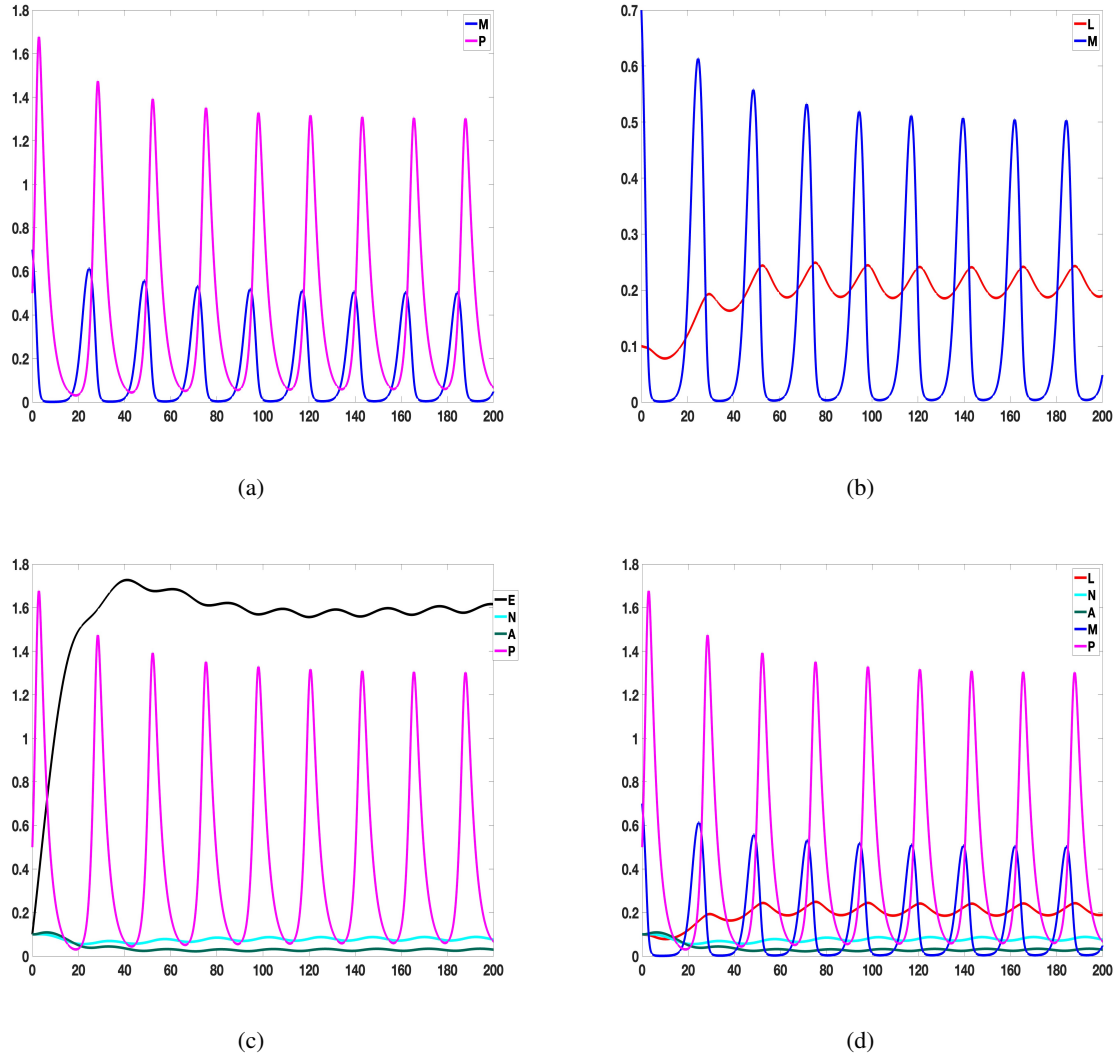

(a) (b)

(c) (d)

Figure 6. Dynamics of the model (3.1) showing the impact of the prey-predator interactions on the tick population. (a) the prey-predator interactions; (b) effect of prey dynamics on larvae population; (c) effect of predator dynamics on the eggs, the nymphs, and adult population; (d) effect of prey-predator dynamics on ticks population.

have significant negative impact on the response functions for the sum of infected ticks $L_I + N_I + A_I$, infected prey (M_I) and infected predator P_I; while the impact of τ is minimal and positive on the sum of infected ticks $L_I + N_I + A_I$, and infected prey (M_I). It is however, has negative impact on P_I. Although the impact of this parameter is low and insignificant, we include this in our simulation because of it's biological importance.

5.2.2. Varying predator attack rate (α_M)

We set the predator attack rate α_M to 0.5, 0.75, 0.95 and simulate model (3.1) to explore the effect of predator attack rate (α_M) on the system. We observed from Figure 8(a) a significant decrease in the

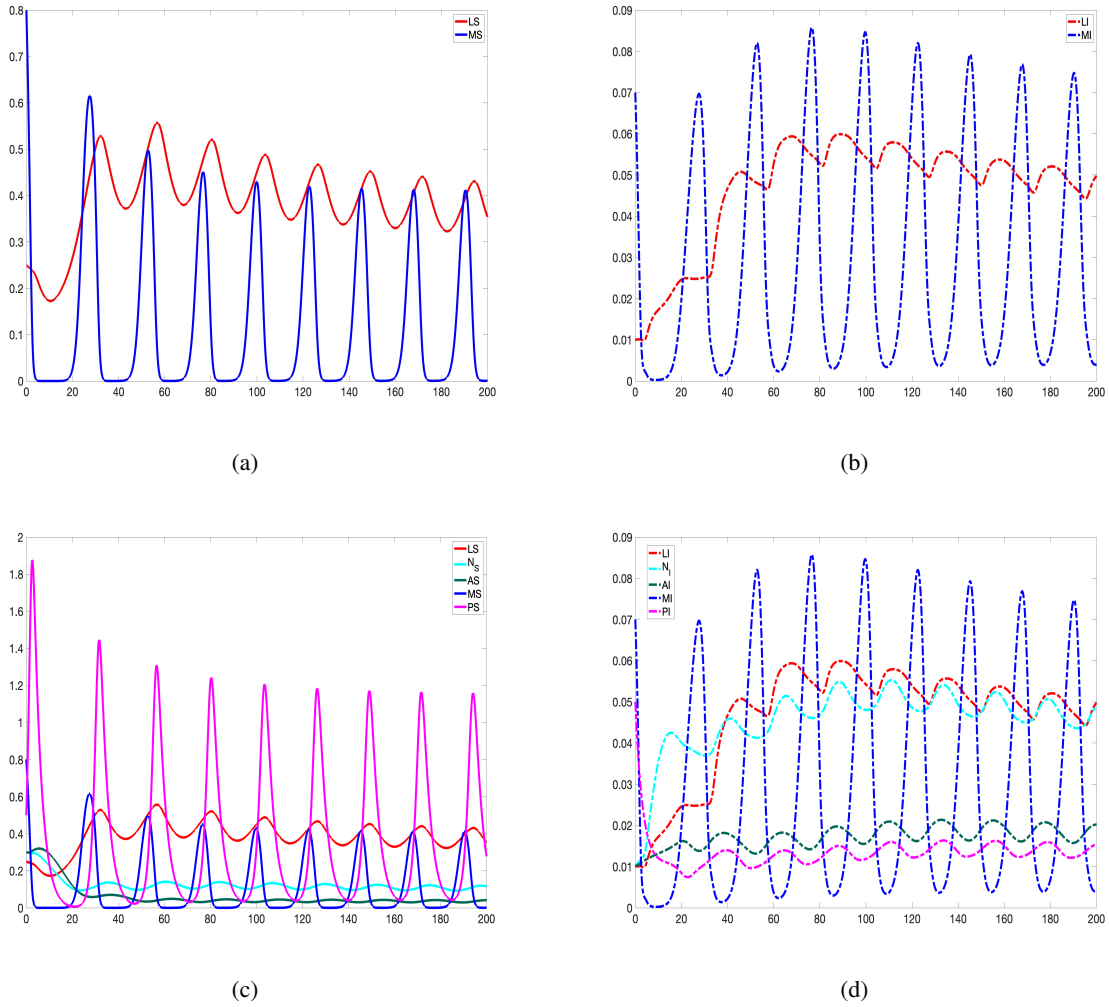

Figure 7. Dynamics of model (2.1) showing the effect of the prey-predator interactions on the tick populations; (a) effect of susceptible prey dynamics on susceptible larvae population; (b) effect of infected prey dynamics on infected larvae population; (c) effect of susceptible prey-predator dynamics on susceptible ticks population; (d) effect of infected prey-predator dynamics on infected ticks population.

susceptible predator population (P) as the attack rate α_M increases with a slight increase in the prey population (M) during the times the prey population increases following a decrease in the predator population. Figure 8(b) show the infected populations. We observed a decrease in both prey and predator populations with increasing attack rate; however, there are more infected prey when the predator are low. Furthermore, we observed in Figures 8(c) and 8(d) the cascading effect of the predator attack on prey who are the hosts to the larvae and nymph tick populations; thus as the attack rate increases we observed a decrease in the tick populations namely the larvae, nymphs, and adults.

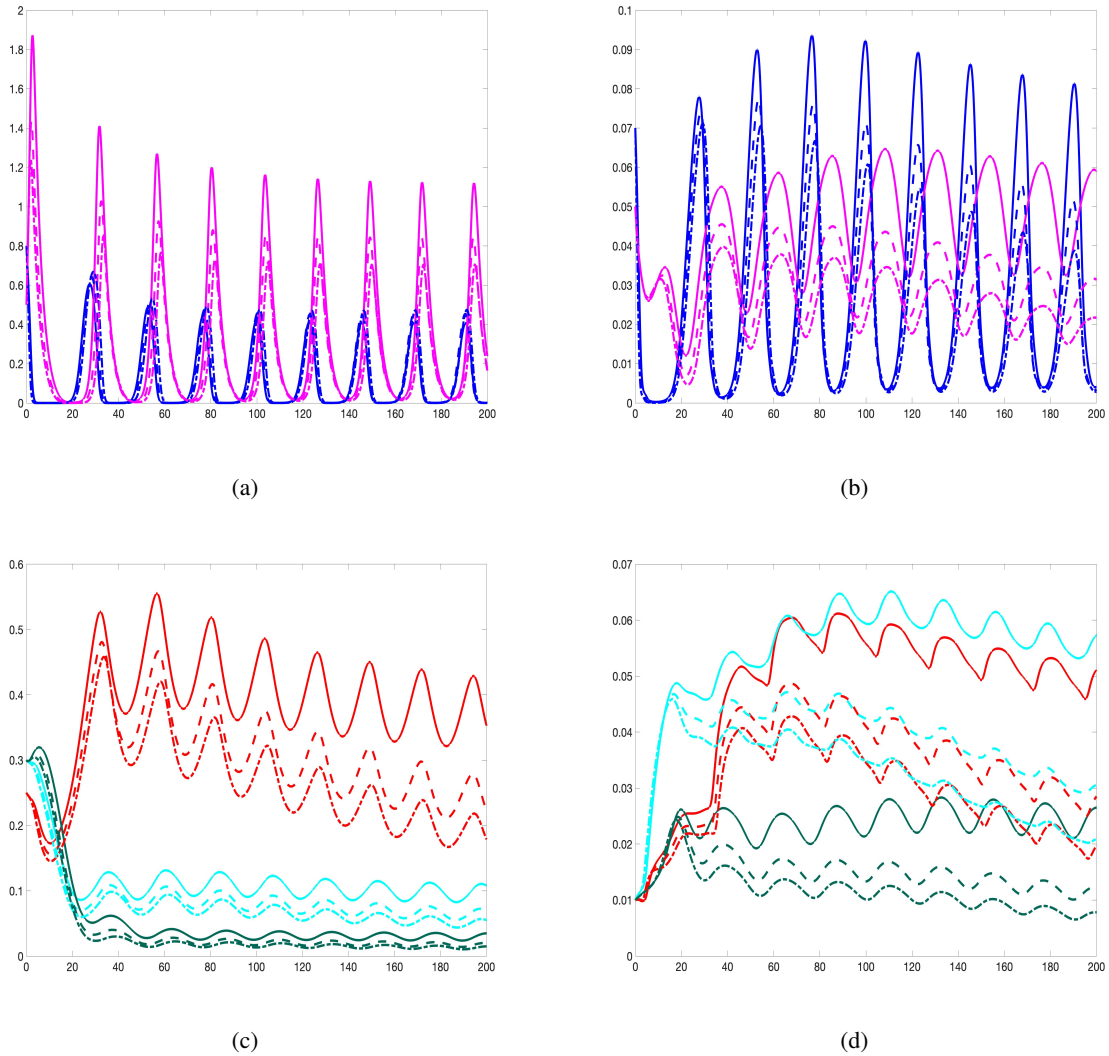

(a) (b)

(c) (d)

Figure 8. Numerical simulations of the ticks-prey-predator model (3.1) varying predator attack rate ($\alpha_M = 0.5, 0.75, 0.95$): (a) susceptible prey and predator; (b) infected prey and predators; (c) susceptible ticks (larvae, nymphs, and adults) (d) infected ticks. Green are larvae, cyan are nymphs, and red are adults. Solid lines represent $\alpha_M = 0.5$, dash lines are $\alpha_M = 0.75$, and dash dot lines represent $\alpha_M = 0.95$.

5.2.3. Varying the fear of the predator (τ)

Next, we vary the fear of the predator and set the fear parameter τ to 1.50, 2.50, 4.50, and simulate model (2.1) to explore the effect of the predator fear rate (τ) on the system. We observed from Figure 9(a) a decrease in the susceptible predator population (P_S) as τ increases with a horizontal shift to the right in the prey population (M_S) when the prey population increases following a decrease in the predator population. Figure 9(b) show the infected populations (P_I, M_I). Both the prey and predator populations decrease with increasing attack rate; however, there are more infected prey when the predator are low. Figures 9(c) and 9(d) shows the cascading effect of the fear of predator on susceptible

and infected tick populations; thus as the fear rate increases, we observed a decrease in larvae, nymphs, and adults tick populations; although this decrease is not as much as what we observed in Figure 8(b) above.

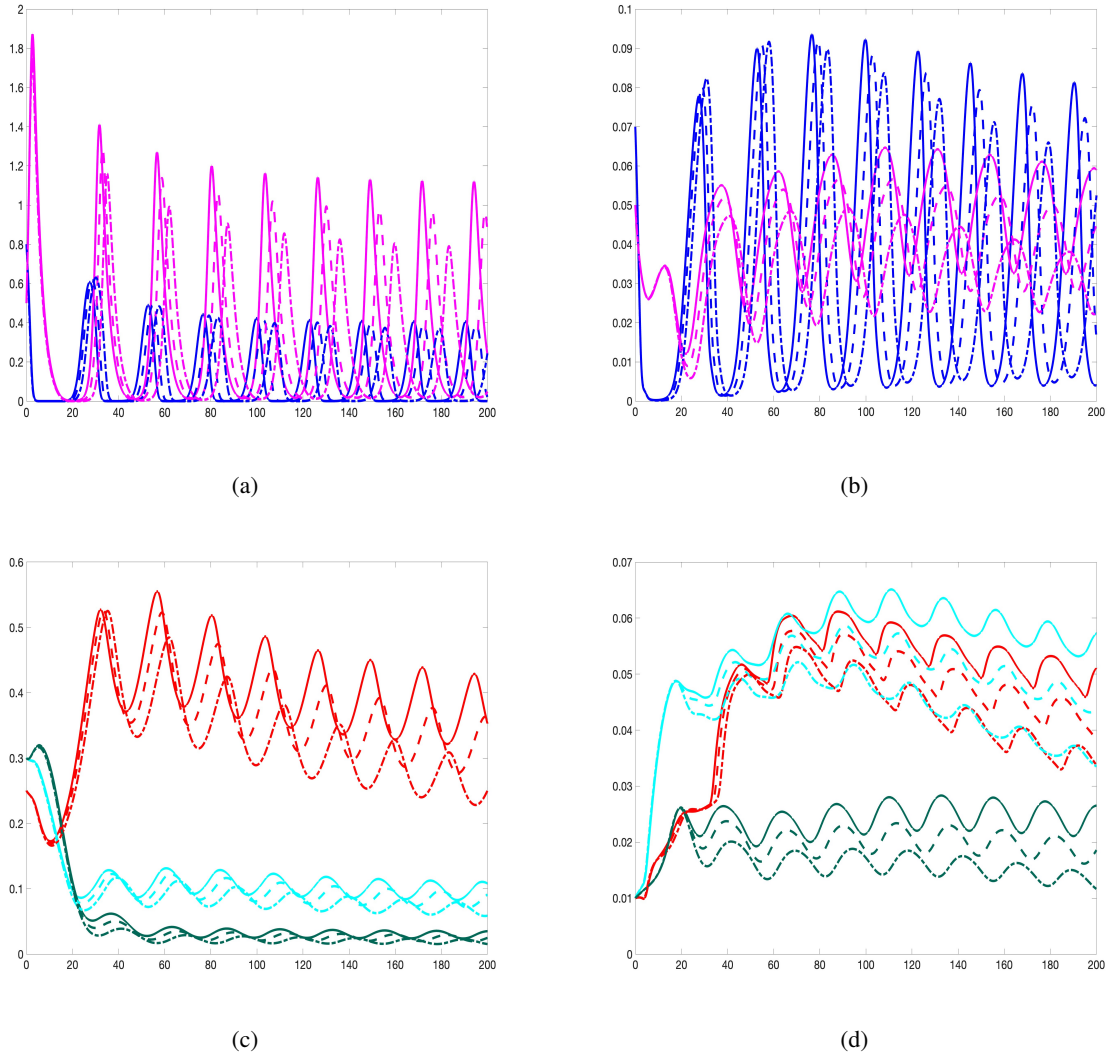

(a) (b)

(c) (d)

Figure 9. Numerical simulations of the ticks-prey-predator model (3.1) varying the fear of the predator (τ) setting $\tau = 1.50, 2.50, 4.50$: (a) susceptible prey and predator; (b) infected prey and predators; (c) susceptible ticks (larvae, nymphs, and adults) (d) infected ticks. Solid lines represent $\tau = 1.50$, dash lines are $\tau = 2.50$, and dash dot lines represent $\tau = 4.50$.

5.2.4. Varying attack (α_M) and fear (τ) rates

Lastly, we vary together the predator attack rate (α_M) and the fear of the predator (τ) and simulate model (2.1) to explore the joint effect of the predator attack rate (α_M) and prey fear rate (τ) on the system. We observed a significant decrease in the susceptible predator population (P_S) in Figure 10(a) as τ increases with a horizontal shift to the right in the susceptible prey population (M_S) at the times

the prey population increases following a decrease in the predator population. Figure 10(b) show the infected populations. We observed a decrease in both prey and predator populations with increasing attack rate; however, there are more infected prey when the predator when the prey are low. We also observed a strong cascading effect of the fear of predator on ticks in Figure 10(c) and 10(d); thus leading to a decrease in the larvae, nymphs, and adults tick populations as the attack and fear rates increases.

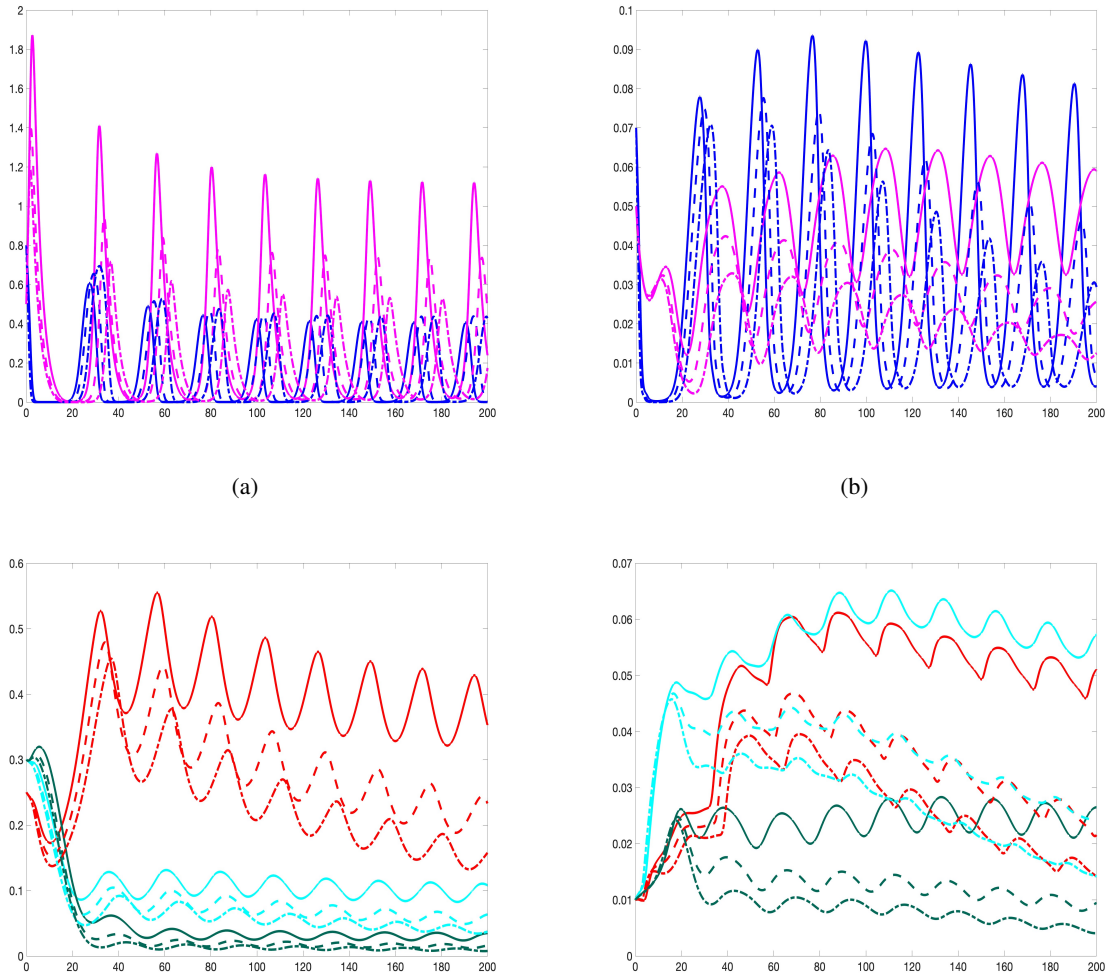

(a) (b)

(c) (d)

Figure 10. Numerical simulations of the ticks-prey-predator model (3.1) varying predators attack rate (α_M) and fear of the predators (τ) setting $\alpha_M = 0.5, 0.75, 0.95$ and $\tau = 1.50, 2.50, 4.50$: (a) infected prey and predators; (b) infected ticks (larvae, nymphs, and adults). Solid lines represent $\alpha_M = 0.5$, $\tau = 1.50$, dash lines are $\alpha_M = 0.75$, $\tau = 2.50$, and dash dot lines represent $\alpha_M = 0.95$, $\tau = 4.50$.

5.2.5. Varying transmission probability (β_{LM})

Next, we vary the probability that a susceptible prey becomes infected from an infectious larvae tick (β_{LM}) and set $\beta_{LM} = 0.018,\ 2 \times 0.018,\ 3 \times 0.0.18$ in Figure 11. We also vary the probability that a susceptible prey and predator becomes infected from an infectious nymphs and adult tick, and vice versa. We then double and triple β_{LM}, β_{NM}, β_{NP}, β_{AP}, β_{PA}, β_{MT}. Although these parameters have low sensitivities index from the sensitivity analysis results. We observed that as the transmission probabilities increases the susceptible populations (host and ticks) decreases and the infected populations increases.

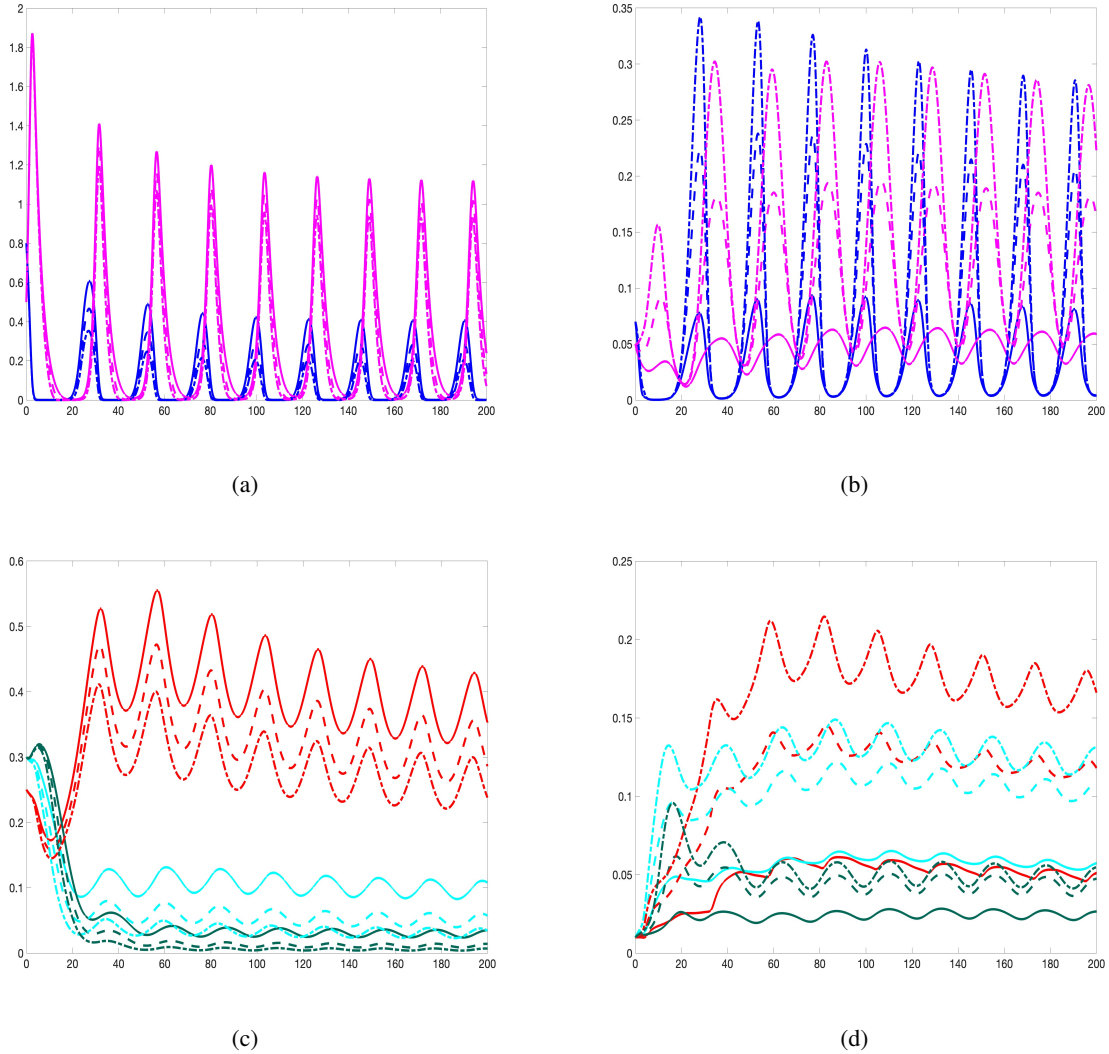

Figure 11. Numerical simulations of the ticks-prey-predator model (3.1) varying predator attack rate (α_M): (a) infected prey and predators; (b) infected ticks (larvae, nymphs, and adults). Solid lines represent $\beta_M = 0.018$, dash lines are $\beta_M = 0.018 \times 2$, and dash dot lines represent $\beta_M = 0.18 \times 3$.

5.2.6. Summary of the simulation scenarios

In this section we ran some simulation scenarios using some of the parameters with the most impact from the sensitivity analysis, specifically we varied the prey-predator parameters α_M (predator attack rate), τ (strength of fear of predators). We also varied the transmission probabilitiesβ_{LM}, β_{NM}, β_{NP}, β_{AP}, β_{PA}, β_{MT}, although these parameters had minimal effect on the response functions used in the sensitivity analysis. We observed a cascading effect of the predator's attack and fear on the prey and the tick populations, since the prey are hosts of the larvae and nymphs. We summarized below the findings from the simulations

(i) Varying predator attack rate (α_M): As the attack rate on the prey increased the tick populations namely the larvae, nymphs, and adults we decreased;
(ii) Varying the fear of the predator (τ): As the fear rate increased, the larvae, nymphs, and adults tick populations decreased;
(iii) Varying transmission probability: As the transmission probabilities increased the infected populations increased leading to a decrease in the susceptible populations both host and ticks alike.

The implications of these results are discussed next in the section below.

6. Discussion

In this paper we developed and analyzed two mathematical models involving ticks-prey-predator interactions model (2.1) with disease and model (3.1) without disease. We use *Erhlichiosis* as our model disease transmitted by ticks, see *Erhlichiosis* model in [24]. The quantitative analysis of model (2.1) with disease transmission, indicate that the disease-free equilibrium is locally asymptotically stable when the reproduction number is less than one and unstable otherwise.

To carry out the quantitative analysis of ticks-prey-predator model (3.1), we first simplify the model. The quantitative analysis of the simplified form using boundedness of the prey and predator indicates that the model has three equilibrium points: tick-only equilibrium, predator-free equilibrium, and co-existence ticks-prey-predator equilibrium. These three equilibrium points are locally asymptotically stable given the conditions in Theorem 3.

Next we carried out a global sensitivity analysis using LHS/PRCC method to determine the parameter with the most influence on the response functions obtained from the ticks-prey-predator model (3.1) without disease. The parameters with the most significant impact on the sum of ticks ($L + N + A$), the prey (M), and the predators (P) are the tick eggs maturation rate (σ_E), the egg carrying capacity (K_E). Other significant parameters are the preys' birth and natural death rate (π_M and μ_M) and their carrying capacity (K_M). The parameter denoting the fear of predators (τ) is equally significant. The last sets of significant parameters are the predator birth and natural death rates (π_P, and μ_P), the predator's attack rate (α_M), and the half saturation constant (a).

We also carried out a global sensitivity analysis using LHS/PRCC method to determine the parameters of the ticks-prey-predator disease model (2.1) with the most influence on the response functions namely the sum of infected ticks ($L_I + N_I + A_I$), infected prey (M_I), and the infected predators (P_I). The most significant parameters for these functions shown in Figure 4 and given in Table 3. These parameters are tick eggs maturation rate (σ_E), the egg carrying capacity (K_E), the probability that a susceptible prey becomes infected from an infectious larvae tick (β_{LM}). The other significant parameters are the

preys birth and natural death rate (π_M and μ_M), and their carrying capacity (K_M). The other equally significant parameters are the predator biomass conversion efficiency (π_P) or predators birth rate, the natural death rate (μ_P), the attack rate (α_M), and the half saturation constant (a). The other parameters are the fear of the predator (τ).

The ticks-prey-predator interactions models (2.1) and (3.1) with and without disease have several significant parameters (like $\sigma_E, K_E, \pi_M, \mu_M, K_M, \pi_P, \mu_P, \alpha_M$, and τ) that are common given the three response functions under consideration. The parameter β_{LM} from model (2.1) is the only parameter not common to both models.

The fear term τ in models (2.1) and (3.1) have variable sensitivity indices for the three response functions. It has a negative impact on the sum of the infected ticks, and the predator, and a positive significant impact on the prey population, although their magnitude if small. This indicate that the effect of fear is negative on the ticks and predator and positive on the prey. This positive effect on the prey we expect is in the short term because studies have show that fear can affect the birth rate of prey population [45], limit foraging activities [46]. For instance, mule deer limit their forage due lion attacks [46]. Thus, in the long run that effect on the prey would be negative since the fear of the predator would prevent them from foraging for food and even mating leading to a decrease in their population over time [45–47].

In Figure 6, we focus on the simulation of the ticks-prey-predator model (3.1) for the unstable prey-predator equilibrium shown in Figure 5(a) to see the effect of the prey-predator interaction on the ticks dynamics. Figure 6(a) shows the prey-predator dynamics. In Figure 6(b), we see that the larvae population follows the trajectory of the prey population, this is due to a number of factors: for instance, the larvae feeds on the prey. Furthermore, the larvae mortality which is density dependent is also dependent on the prey population; hence, the larvae population decreases with the prey population and increases when the prey population increases. We also observed in Figure 6(c) that the nymphs and the adult follow the predator population trajectory since the egg laying rate, nymph, and adult mortality both depends on the predator population. Additionally, the nymph population also depends on the prey population. However, from our numerical simulations, we observed dominance by the predator population in terms of following the trajectory. This is quite interesting and worthy of further investigation to ascertain the true cause of dominance by the predator population. This observation substantiate the results obtained in [48]. Although this interactions is between coral reef fishes; however, the authors emphasized the importance of predation and competition within hierarchies between two coral reef fishes.

Considering the effect of varying the predators attack rate (α_M) is crucial in understanding disease outbreaks within the populations. In Figure 11, we investigate how changes in the predators attack rate impact disease transmission. By adjusting α_M from 0.5 to 0.95, we observed distinct outcomes. We observed in Figure 8(a) a decline in the populations of infected larvae, nymphs, and adult ticks as the predators attack rate on the prey increases. This decline indicates that the infected predators play a significant role in reducing the prevalence of tick-borne diseases by preying on the infected ticks. Consequently, the overall tick burden decreases, leading to a potential reduction in disease transmission to hosts. This observation from our numerical simulations substantiate experimental results in ecology where predators and competitors of vertebrates can in theory reduce the density of infected nymphs [18], and thus may have a cascading impacts on the tick-borne disease risk. However, in Figure 8(b), we observe a different trend. Here, despite the increase in predator activity, we notice a decrease in

the predator population and a marginal rise in the prey population. This unexpected outcome suggests a possible trade-off between predator survival and prey control efficiency. The decline in the infected predator population might be attributed to the additional time and energy expended in intensifying attacks on infected prey individuals. As a result, while predator activity may initially reduce disease prevalence, sustained high attack rates could lead to a decline in predator fitness, potentially impacting long-term disease regulation dynamics.

The non-lethal effect of predation due to fear (τ) is further explored in Figure 9. We observed a decline and shift in the dynamics of the infected ticks populations, i.e., larvae, nymphs, and adult ticks as the strength of fear parameter increases, see Figure 9(a). This observation indicates that intensifying the strength of fear of infected predators among infected prey populations lead to a decrease in tick burden within the ecosystem, thus a cascading effects on the tick-borne disease risks. Also, in Figure 9(b), we observed a decrease and shift in the infected predator populations and a slight decrease in the population of the infected prey. These could be due to several factors. Intensifying the strength fear of predators may have resulted in reduced encounter rates between infected predators and infected prey, limiting opportunities for predation and thus impacting the infected predator populations. In a related study [49], researchers found similar results. They noticed that as the fear of predation increased, the predator population decreased, and in some cases, high levels of fear even caused the predators to become extinct. Additionally, an increase in the strength of fear (τ) could lead to changes in infected predator behavior, such as decreased hunting efficiency. Conversely, the slight decrease in infected prey populations may be as a result from a combination of reduced predation pressure and altered prey behavior in response to fear. The infected prey populations may exhibit avoidance behaviors or alter their habitat use patterns to reduce encounters with infected predators, leading to a decrease in infected prey densities over time [50] .

In Figure 10, we carried out numerical simulations where we simultaneously increased both the infected predators' attack rate (α_M) and the strength of infected predators fear (τ) to observe their combined impact on the dynamics of the system. Our observations revealed a trend consistent with the findings from individual parameter variations. As we increased both α_M and τ simultaneously, we observed a decrease in the populations of infected larvae, nymphs, and adult ticks, see Figure 10(a). Similarly, we observed a decline and a shift in the predators population. Therefore, the combined effect of predators attack rate and the intensity of fear can have intricate consequences on populations of infected prey and predators, consequently influencing the risk of tick-borne diseases.

7. Conclusion

To conclude, in this study we developed a deterministic model of ordinary differential equations to gain insight on the effect of prey-predator interaction and the cascading effect of fear of the predators on ticks population and disease prevalence. We found that tick host predator and fear of the predators reduces the tick populations and disease prevalence. We summarize the other results as follows:

(i) The results of the Sensitivity analyzes was implemented using three response or output functions namely the sum of infected ticks ($L_I + N_I + A_I$), infected predators (M_I), and the infected predators (P_I) to identify the parameters with the most impact on these functions in no particular order. The most significant common parameters among these functions are the eggs maturation rates (σ_E), and carrying capacity (K_E). Other significant parameters are the preys birth and natural death

rates (π_M, μ_M). The last sets of significant common parameters are the predator birth and natural death rates (π_P, and μ_P), the predator's attack rate (α_M), and the half saturation constant (a). The probability that a susceptible prey becomes infected from an infectious larvae tick (β_{LM}) is also a significant parameter.

(ii) The trajectory of the susceptible larvae population follow the trajectory of the susceptible prey population. While susceptible nymphs and adults follow the trajectories of susceptible predator. The trajectories of the nymphs and adult population either susceptible or infected follow the trajectory of the predator population (susceptible or infected).

(iii) There are more infected larvae when infected prey population are low and few infected larvae when there are more infected prey. Similar dynamics was observed for the infected nymphs and adult ticks and infected predator population.

(iv) Prey predation and fear of predator have cascading effect on tick populations and disease prevalence. As prey attack rate increases, there is corresponding reduction in the prey and ticks population; furthermore as the fear of the predator increases we observed a reduction in the prey population which subsequently lead to a decrease in the ticks populations.

In this study, we have used mathematical models to investigate the cascading effect of prey-predator interaction and predator fear tick populations and disease prevalence. One of the limitations of this study is not including additional source of food for the predator. We know that often times, the predator have other sources of food aside from the prey populations, see [51] and references therein. Another limitation of the study is that we were not specific as to the kind of prey population we are interested in; however, tick larvae and nymphs are known to feed on small mammals while the adult ticks feed on much larger mammals including the predators which we capture in the two models in this study. Another major drawback was the availability of data. Although, we have off set this drawback by using parameter estimates from literature; we are confident in our conclusions since are results are backed up by the outcomes obtained from the sensitivity analysis we carried out.

Use of AI tools declaration

The authors declare they have not used Artificial Intelligence (AI) tools in the creation of this article.

Acknowledgments

This material is based upon work supported by the National Science Foundation (NSF) under Grant No. DMS-1928930, National Security Agency (NSA) under Grant No. H98230-23-1-0012 and the Sloan Foundation under Grant G-2020-14104 while the author participated in ADJOINT hosted by the Mathematical Sciences Research Institute in Berkeley, California, in [2023-2024]. FBA had additional support from the National Science Foundation under the EPSCOR Track 2 grant number 1920946.

Conflict of interest

The authors declare there is no conflict of interest.

References

1. J. S. Bakken, The discovery of human granulocytotropic ehrlichiosis, *J. Labor. Clin. Med.*, **132** (1988), 175–180. https://doi.org/10.1016/S0022-2143(98)90165-2V
2. Centers for Disease Control and Prevention (CDC), *Ehrlichiosis*, 2022. Available from: `https://www.cdc.gov/ehrlichiosis/`
3. J. Goddard, A. S. Varela-Stokes, Role of the lone star tick, amblyomma americanum (l.), in human and animal diseases, *Vet. Parasitol.*, **160** (2009), 1–12. https://doi.org/10.1016/j.vetpar.2008.10.089
4. L. Eisen, Tick species infesting humans in the united states, *Ticks Tick-borne Diseases*, **13** (2022), 102025. https://doi.org/10.1016/j.ttbdis.2022.102025
5. H. A. Merten, L. A. Durden, A state-by-state survey of ticks recorded from humans in the united states, *J. Vector Ecol. J. Soc. Vector Ecol.*, **25** (2000), 102–113.
6. D. E. Sonenshine, R. M. Roe, *Biology of ticks volume 2*, Oxford University Press, 2014.
7. B. F. Allan, F. Keesing, R. S. Ostfeld, Effect of forest fragmentation on lyme disease risk, *Conserv. Biol.*, **17** (2003), 267–272. https://doi.org/10.1046/j.1523-1739.2003.01260.x
8. J. E. Childs, C. D. Paddock, The ascendancy of amblyomma americanum as a vector of pathogens affecting humans in the united states, *Ann. Rev. Entomol.*, **48** (2003), 307–337. https://doi.org/10.1146/annurev.ento.48.091801.112728
9. R. S. Ostfeld, R. D. Holt, Are predators good for your health? evaluating evidence for top-down regulation of zoonotic disease reservoirs, *Front. Ecol. Environ.*, **2** (2004), 13–20. https://doi.org/10.1890/1540-9295(2004)002[0013:APGFYH]2.0.CO;2
10. A. Bourdin, S. Bord, J. Durand, C. Galon, S. Moutailler, M. Scherer-Lorenzen, et al., Forest diversity reduces the prevalence of pathogens transmitted by the tick ixodes ricinus, *Front. Ecol. Evolut.*, **10** (2022), 891908. https://doi.org/10.3389/fevo.2022.891908
11. L. K. Lindsø, H. Viljugrein, A. Mysterud, Temporal increase in ticks and pathogen prevalence in the small mammal part of the lyme disease cycle in northern europe, *Ecosphere*, **15** (2024), e70063. https://doi.org/10.1002/ecs2.70063
12. K. LoGiudice, R. S. Ostfeld, K. A. Schmidt, F. Keesing, The ecology of infectious disease: Effects of host diversity and community composition on lyme disease risk, *Proceed. Nat. Acad. Sci.*, **100** (2003), 567–571. https://doi.org/10.1073/pnas.0233733100
13. K. D. McCoy, E. Léger, M. Dietrich, Host specialization in ticks and transmission of tick-borne diseases: A review, *Front. Cellular Infect. Microbiol.*, **3** (2013), 57. https://doi.org/10.3389/fcimb.2013.00057
14. E. L. Preisser, D. I. Bolnick, M. F. Benard, Scared to death? the effects of intimidation and consumption in predator–prey interactions, *Ecology*, **86** (2005), 501–509. https://doi.org/10.1890/04-0719
15. A. Fritzsche, B. F. Allan, The ecology of fear: Host foraging behavior varies with the spatio-temporal abundance of a dominant ectoparasite, *EcoHealth*, **9** (2012), 70–74. https://doi.org/10.1007/s10393-012-0744-z

16. D. W. Thieltges, P. T. Johnson, A. van Leeuwen, J. Koprivnikar, Effects of predation risk on parasite–host interactions and wildlife diseases, *Ecology*, **105** (2024), e4315. https://doi.org/10.1002/ecy.4315

17. S. A. Adamo, R. H. Easy, I. Kovalko, J. MacDonald, A. McKeen, T. Swanburg, et al., Predator exposure-induced immunosuppression: Trade-off, immune redistribution or immune reconfiguration?, *J. Exper. Biol.*, **220** (2017), 868–875. https://doi.org/10.1242/jeb.153320

18. T. R. Hofmeester, P. A. Jansen, H. J. Wijnen, E. C. Coipan, M. Fonville, H. H. Prins, et al., Cascading effects of predator activity on tick-borne disease risk, *Proceed. Royal Soc. B Biol. Sci.*, **284** (2017), 20170453. https://doi.org/10.1098/rspb.2017.0453

19. T. Levi, A. M. Kilpatrick, M. Mangel, C. C. Wilmers, Deer, predators, and the emergence of lyme disease, *Proceed. Nat. Acad. Sci.*, **109** (2012), 10942–10947. https://doi.org/10.1073/pnas.1204536109

20. X. Wang, L. Zanette, X. Zou, Modelling the fear effect in predator–prey interactions, *J. Math. Biol.*, **73** (2016), 1179–1204. https://doi.org/10.1007/s00285-016-0989-1

21. M. Hossain, N. Pal, S. Samanta, Impact of fear on an eco-epidemiological model, *Chaos Solit. Fract.*, **134** (2020), 109718. https://doi.org/10.1016/j.chaos.2020.109718

22. C. Zhang, The effect of the fear factor on the dynamics of an eco-epidemiological system with standard incidence rate, *Infect. Disease Model.*, **9** (2024), 128–141. https://doi.org/10.1016/j.idm.2023.12.002

23. A. K. Pribadi, S. H. Chalasani, Fear conditioning in invertebrates, *Front. Behav. Neurosci.*, **16** (2022), 1008818. https://doi.org/10.3389/fnbeh.2022.1008818

24. F. Alexander, F. B. Agusto, *Effects of rising temperature and prescribed fire on Amblyomma Americanum with ehrlichiosis*, in *Mathematical and Computational Modeling of Phenomena Arising in Population Biology and Nonlinear Oscillations*(Ed. Abba Gumel), American Mathematical Society, 2023.

25. A. Ludwig, H. S. Ginsberg, G. J. Hickling, N. H. Ogden, A dynamic population model to investigate effects of climate and climate-independent factors on the lifecycle of amblyomma americanum (acari: Ixodidae), *J. Med. Entomol.*, **53** (2016), 99–115. https://doi.org/10.1093/jme/tjv150

26. D. Wallace, V. Ratti, A. Kodali, J. M. Winter, M. P. Ayres, J. W. Chipman, et al., Effect of rising temperature on lyme disease: Ixodes scapularis population dynamics and borrelia burgdorferi transmission and prevalence, *Canadian J. Infect. Diseases Med. Microbiol.*, **2019** (2019), 9817930. https://doi.org/10.1155/2019/9817930

27. R. Rosà, A. Pugliese, Effects of tick population dynamics and host densities on the persistence of tick-borne infections, *Math. Biosci.*, **208** (2007), 216–240. https://doi.org/10.1016/j.mbs.2006.10.002

28. X. Zhang, B. Sun,Y. Lou, Dynamics of a periodic tick-borne disease model with co-feeding and multiple patches, *J. Math. Biol.*, **82** (2021), 27. https://doi.org/10.1007/s00285-021-01582-6

29. E. Guo, F. B. Agusto, Baptism of fire: Modeling the effects of prescribed fire on lyme disease, *Canadian J. Infect. Diseases Med. Microbiol.*, **2022** (2022), 5300887. https://doi.org/10.1155/2022/5300887

30. P. Van den Driessche, J. Watmough, Reproduction numbers and sub-threshold endemic equilibria for compartmental models of disease transmission, *Math. Biosci.*, **180** (2002), 29–48. https://doi.org/10.1016/S0025-5564(02)00108-6

31. R. M. Anderson, R. M. May, *Infectious diseases of humans: dynamics and control*, Oxford university press, 1991. https://doi.org/10.1093/oso/9780198545996.001.0001

32. O. Diekmann, J. A. P. Heesterbeek, J. A. J. Metz, On the definition and the computation of the basic reproduction ratio r 0 in models for infectious diseases in heterogeneous populations, *J. Math. Biol.*, **28** (1990), 365–382. https://doi.org/10.1007/BF00178324

33. H. W. Hethcote, The mathematics of infectious diseases, *SIAM Rev.*, **42** (2000), 599–653. https://doi.org/10.1137/S0036144500371907

34. S. Chen, F. Chen, V. Srivastava, R. D. Parshad, Dynamical analysis of an allelopathic phytoplankton model with fear effect, *Qualit. Theory Dynam. Syst.*, **23** (2024), 189. https://doi.org/10.1007/s12346-024-01047-3

35. H. Zhang, Y. Cai, S. Fu, W. Wang, Impact of the fear effect in a prey-predator model incorporating a prey refuge, *Appl. Math. Comput.*, **356** (2019), 328–337. https://doi.org/10.1016/j.cam.2019.01.034

36. K. Antwi-Fordjour, S. P. Westmoreland, K. H. Bearden, Dual fear phenomenon in an eco-epidemiological model with prey aggregation, *European Phys. J. Plus*, **139** (2024), 518. https://doi.org/10.1140/epjp/s13360-024-05324-7

37. S. Pal, N. Pal, S. Samanta, J. Chattopadhyay, Effect of hunting cooperation and fear in a predator-prey model, *Ecol. Complex.*, **39** (2019), 100770. https://doi.org/10.1016/j.ecocom.2019.100770

38. V. Srivastava, K. Antwi-Fordjour, R. D. Parshad, Exploring unique dynamics in a predator–prey model with generalist predator and group defense in prey, *Chaos*, **34** (2024). https://doi.org/10.1063/5.0171950

39. S. K. Sasmal, Y. Takeuchi, Dynamics of a predator-prey system with fear and group defense, *J. Math. Anal. Appl.*, **481** (2020), 123471. https://doi.org/10.1016/j.jmaa.2019.123471

40. Centers for Disease Control and Prevention (CDC), How ticks spread disease, Accessed August 7 2023. Available from: `https://www.cdc.gov/ticks/life_cycle_and_hosts.html`

41. S. M. Blower, H. Dowlatabadi, Sensitivity and uncertainty analysis of complex models of disease transmission: An HIV model, as an example, *Int. Stat. Rev.*, (1994), 229–243. https://doi.org/10.2307/1403510

42. S. Marino, I. B. Hogue, C. J. Ray, D. E. Kirschner, A methodology for performing global uncertainty and sensitivity analysis in systems biology, *J. Theor. Biol.*, **254** (2008), 178–196. https://doi.org/10.1016/j.jtbi.2008.04.011

43. M. D. McKay, R. J. Beckman, W. J. Conover, A comparison of three methods for selecting values of input variables in the analysis of output from a computer code, *Technometrics*, **42** (2000), 55–61. https://doi.org/10.1080/00401706.2000.10485979

44. M. A. Sanchez, S. M. Blower, Uncertainty and sensitivity analysis of the basic reproductive rate: Tuberculosis as an example, *Am. J. Epidemiol.*, **145** (1997), 1127–1137. https://doi.org/10.1093/oxfordjournals.aje.a009076

45. D. Mukherjee, Study of fear mechanism in predator-prey system in the presence of competitor for the prey, *Ecol. Genet. Genom.*, **15** (2020), 100052. https://doi.org/10.1016/j.egg.2020.100052

46. K. B. Altendorf, J. W. Laundré, C. A. López González, J. S. Brown, Assessing effects of predation risk on foraging behavior of mule deer, *J. Mammal.*, **82** (2001), 430–439. https://doi.org/10.1644/1545-1542(2001)082¡0430:AEOPRO¿2.0.CO;2

47. K. Sarkar, S. Khajanchi, Spatiotemporal dynamics of a predator-prey system with fear effect, *J. Franklin Institute*, **360** (2023), 7380–7414. https://doi.org/10.1016/j.jfranklin.2023.05.034

48. A. Hall, M. Kingsford, Predators exacerbate competitive interactions and dominance hierarchies between two coral reef fishes, *PLoS One*, **11** (2016), e0151778. https://doi.org/10.1371/journal.pone.0151778

49. P. Panday, N. Pal, S. Samanta, P. Tryjanowski, J. Chattopadhyay, Dynamics of a stage-structured predator-prey model: Cost and benefit of fear-induced group defense, *J. Theor. Biol.*, **528** (2021), 110846. https://doi.org/10.1016/j.jtbi.2021.110846

50. S. L. Hermann, D. A. Landis, Scaling up our understanding of non-consumptive effects in insect systems, *Current Opinion Insect Sci.*, **20** (2017), 54–60. https://doi.org/10.1016/j.cois.2017.03.010

51. R. D. Parshad, S. Wickramasooriya, K. Antwi-Fordjour, A. Banerjee, Additional food causes predators to explode—unless the predators compete, *Int. J. Bifurc. Chaos*, **33** (2023), 2350034. https://doi.org/10.1142/S0218127423500347

AIMS Press